NAVAL POSTGRADUATE SCHOOL
MONTEREY, CALIFORNIA

THESIS

THE INSTRUMENTATION DESIGN AND CONTROL OF A T63-A-700 GAS TURBINE ENGINE

by

David Williams Haas

June, 1996

Thesis Advisor: Knox T. Millsaps, Jr.

Approved for public release; distribution is unlimited.

REPORT DOCUMENTATION PAGE

Form Approved OMB No. 0704-0188

1. AGENCY USE ONLY *(Leave blank)*	2. REPORT DATE	3. REPORT TYPE AND DATES COVERED
	June 1996	Master's Thesis

4. THE INSTRUMENTATION DESIGN AND CONTROL OF A T63-A-700 GAS TURBINE ENGINE	5. FUNDING NUMBERS
6. AUTHOR(S) David W. Haas	
7. PERFORMING ORGANIZATION NAME(S) AND ADDRESS(ES) Naval Postgraduate School Monterey CA 93943-5000	8. PERFORMING ORGANIZATION REPORT NUMBER
9. SPONSORING/MONITORING AGENCY NAME(S) AND ADDRESS(ES)	10. SPONSORING/MONITORING AGENCY REPORT NUMBER
11. SUPPLEMENTARY NOTES The views expressed in this thesis are those of the author and do not reflect the official policy or position of the Department of Defense or the U.S. Government.	
12a. DISTRIBUTION/AVAILABILITY STATEMENT Approved for public release; distribution is unlimited.	12b. DISTRIBUTION CODE

13. ABSTRACT *(maximum 200 words)*

A T63-A-700 gas turbine engine has been instrumented to measure performance parameters. Pressure and temperature monitoring systems have been designed, fabricated, and installed to ensure accurate measurement of performance parameters. All measured parameters have been compared against predicted thermodynamic cycle analysis. Design and control of selected engine systems have been modified to incorporate more precise engine control and safety.

14. SUBJECT TERMS Gas Turbine Instrumentation and Control			15. NUMBER OF PAGES 139
			16. PRICE CODE
17. SECURITY CLASSIFICATION OF REPORT Unclassified	18. SECURITY CLASSIFICATION OF THIS PAGE Unclassified	19. SECURITY CLASSIFICATION OF ABSTRACT Unclassified	20. LIMITATION OF ABSTRACT UL

NSN 7540-01-280-5500

Standard Form 298 (Rev. 2-89)
Prescribed by ANSI Std. 239-18 298-102

Approved for public release; distribution is unlimited.

THE INSTRUMENTATION DESIGN AND CONTROL OF A T63-A-700 GAS TURBINE ENGINE

David W. Haas
Lieutenant, United States Navy
B.S., United States Naval Academy, 1990

Submitted in partial fulfillment
of the requirements for the degree of

MASTER OF SCIENCE IN MECHANICAL ENGINEERING

from the

NAVAL POSTGRADUATE SCHOOL
June 1996

ABSTRACT

A T63-A-700 gas turbine engine has been instrumented to measure performance parameters. Pressure and temperature monitoring systems have been designed, fabricated, and installed to ensure accurate measurement of performance parameters. All measured parameters have been compared against predicted thermodynamic cycle analysis. Design and control of selected engine systems have been modified to incorporate more precise engine control and safety.

TABLE OF CONTENTS

I. INTRODUCTION

Gas turbine engines are widely used in both military and industrial applications. Today, gas turbine engines are found on all major surface combatants and aircraft in the United States Navy. With such a large volume of ships and aircraft in the Navy's arsenal being powered by gas turbine engines, it is natural that the Naval Postgraduate School should study their design and applications.

To this end, a gas turbine engine is necessary to support thesis research and course laboratories; specifically, to investigate advanced measurement techniques for gas turbines such as optical flow measurement, emissions, joint time frequency analysis of vibration signals, and to demonstrate the actual thermodynamics of a real Brayton cycle. The motivation for undertaking such a project is twofold. First, the previous gas turbine engine, a Boeing 502-6A, was in service for over 25 years at the Naval Postgraduate School and in need of replacement. Second, the engine cycle analysis of the Boeing 502 had many problems, including: erroneous state point measurements which led to inaccurate component efficiency computation, lack of instrumentation, and engine control malfunctions. A gas turbine test cell was designed and built in the new Mechanical Engineering building, and an Allison T63-A-700 (250-C18 civilian equivalent) gas turbine engine was chosen for laboratory operations.

The objectives of this thesis are:

1. To accurately instrument all major engine components, support systems, and engine cell parameters in order to accurately asses component behavior and operating conditions.

2. To safely and precisely control the engine and its supporting auxiliary equipment.

Chapter II provides a brief description of the Allison T63-A-700 gas turbine engine along with basic performance data and the engine's leading particulars.

The production model T63-A-700 gas turbine engine instrumentation is not sufficient for thorough performance evaluation. The instrumentation requirements for engine performance analysis are discussed in Chapter III. Additionally, an uncertainty analysis for major component efficiency calculations is addressed.

Chapter IV discusses the instrumentation systems that were designed, fabricated, and installed to adequately measure engine performance, using the requirements discussed in Chapter III for engine performance analysis.

Chapter V addresses the subject of engine control systems to include engine speed, load control, and support systems. Standard Operating Procedures, which were written to ensure safe operation, are evaluated and verified.

Chapter VI explains the methods used for verifying that the instrumentation package accurately measures component and engine behavior. This is accomplished by

testing the engine and comparing the test results against both the gas turbine engine installation manual and predicted thermodynamic models. Additionally, checks for consistency of measurement are accomplished by comparing the results of separate, but redundant instrumentation systems.

In Chapter VII a summary of the overall systems control and instrumentation package, along with its limitations, are discussed. Recommendations for future work are provided.

II. ENGINE DESCRIPTION

The gas turbine engine installed in the Marine Propulsion Laboratory is a Model 250-C18 / T63-A-700 (military) turboshaft engine manufactured by Allison Division, Rolls Royce Corporation of Indianapolis, Indiana (Figure 2.1). Weighing only 138 pounds it is considered a relatively small gas turbine engine and its principal military use was in the U.S. Army's OH-58 light observation helicopter. Over 25,000 engines of this type were manufactured by Allison with nearly 5,000 being delivered to the U.S. Military, making this engine one of the most widely produced gas turbines.

The engine is designed to generate a maximum of 317 SHP at 51,600 (105% design) gas generator turbine RPM and 35,000 power turbine RPM, gearing down to 6,000 RPM at the engine output drive spline. However, due to high engine temperatures at 317 SHP, this power level is used only for takeoff and limited to a total of five minutes. The maximum continuous power level is 270 SHP (100% design). Here the gas producer speed is 49,760 RPM and the power turbine is still maintained at 35,000 RPM. During takeoff the specific fuel consumption is 0.697 lbm/SHP-hr and increases to 0.706 lbm/SHP-hr for the maximum continuous power setting. Table 2.1 and Table 2.2 contain all of the T63-A-700 leading particulars.

The engine consists of four primary sections: the compressor, the combustor, the gas generator turbine, and the power turbine. Air enters the compressor, which consists of six axial stages followed by one centrifugal stage. The overall compressor pressure ratio is 6.2:1 at full power. The air is then discharged from the compressor through a scroll

type diffuser into two circular ducts which direct it into the rear of the engine. The air flow is then reversed into a single combustion chamber. A single fuel nozzle sprays atomized fuel into the combustion chamber where it mixes with the air and combustion occurs. Also located in the combustion chamber is a single exciter ignitor plug which is energized only during start.

The hot combustion gases next enter the turbines. First, the gas generator turbine is encountered. This turbine is an axial two-stage turbine which directly drives the compressor and also an accessories gear train. The accessories gear train provides input power to the fuel pump and gas generator fuel control as well as the lube oil supply and scavenge pumps. The gas generator turbine is aerodynamically coupled to the power turbine. The power turbine is also an axial, two stage design. This turbine is coupled to a helical reduction gear in the power turbine accessories gear box which reduces the power turbine speed of 35,000 RPM to an output RPM of 6,000 at the drive spline.

Dimensions:	
Length	40.4 IN (1.03 m)
Height	22.5 IN (0.57 m)
Width	19.0 IN (0.48 m)
Engine weight (dry):	
T63-A-700	138.5 LB (62.82 kg)
Maximum oil consumption:	0.05 GAL/HR (0.19 L/HR)
Lubricating oil specifications:	MIL-L-23699 or MIL-L-7808
Oil pressure limits:	
97% N_1 speed and above	110-130 (PSIG)
78% to 97% N_1 speed	90-130 (PSIG)
Below 78% N_1 speed	50 (PSIG minimum)
Oil inlet temperature:	
Maximum	225 F
Desired operating range	140-225 F
Fuel specifications:	
Primary	MIL-T-5624 (JP-4)
Alternate	MIL-T-5624 (JP-5) (JP-8) (JET-A)
(JETA-1) (Diesel Fuel NR 2)	
Design power output:	317 SHP
Ram power rating	335 SHP
Design speeds:	
Gas producer (N1)	100% (51,120 RPM)
Power turbine (N2)	100% (35,000 RPM)
Power output shaft	100% (6,000 RPM)
Over speed limits:	
Gas Producer	
Maximum continuous	104% (53,164 RPM)
Maximum overspeed (15 sec max)	105% (53,676 RPM)
Maximum measured gas temperature:	1,380 F (@ Power Turbine Inlet)
Maximum output shaft torque:	
Transients (less than 10 seconds)	320 (LB-FT)
Takeoff (less than 5 minutes)	293 (LB-FT)
Maximum continuous	249 (LB-FT)

Table 2.1. Leading Particulars [Ref. 1: p. 1-22 through 1-23].

Rating	Shaft Horsepower (HP)	Gas Generator Speed (RPM)	Output Shaft Speed (RPM)	Air Flow (SCFM)	Specific Fuel Consumption (LB/SHP-HR)
105%	317	51,600	6,000	2,600	0.697
95%	243	48,650	6,000	2,150	0.725
92%	203	46,950	6,000	1,685	0.762
Start and Idle	35	32,000	4,300		1.743

Table 2.2. T63-A-700 Performance Ratings [Ref. 1: p.1-2].

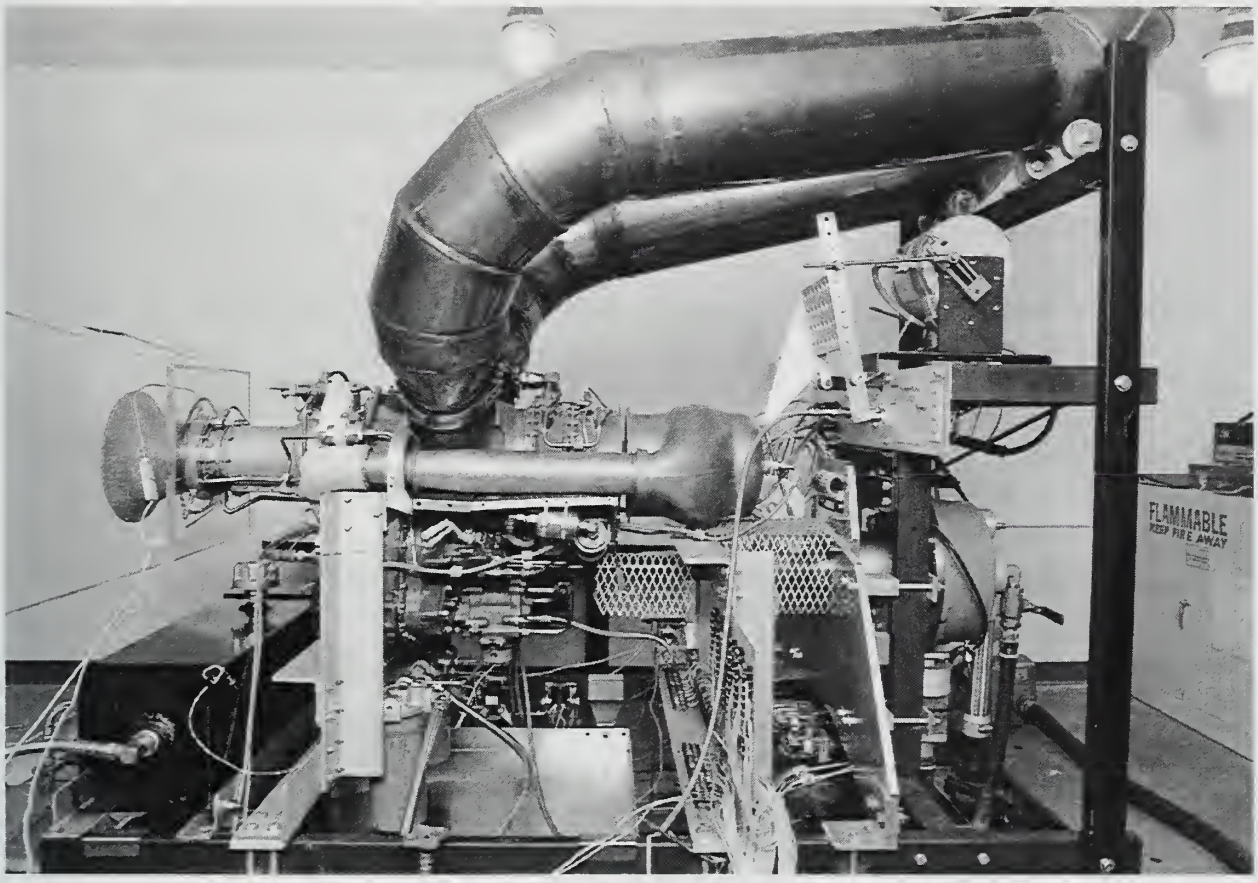

Figure 2.1. T63-A-700 Gas Turbine Engine.

III. INSTRUMENTATION REQUIREMENTS

The onboard engine instrumentation installed on the T63-A-700 gas turbine engine is not sufficient to conduct accurate thermodynamic analysis of engine components and determine engine output performance. Additional instrumentation is necessary to provide information on state points and flow conditions.

A. QUANTITIES TO MEASURE

Initially, the built-in instrumentation package on the gas turbine engine included:

1. Power Turbine (PT) inlet temperature (T_{T5}).
2. Gas Generator Turbine (GGT) / Compressor and Power Turbine (PT) RPM tachometers.
3. Compressor discharge pressure (CDP) for fuel governor control.

Engine performance and component analysis cannot be accomplished with such limited instrumentation. To this end, the performance of the gas turbine engine can be described in specific calculated parameters. The following measured quantities are to be determined for the T63-A-700 gas turbine engine. The symbol used to identify the parameter is in parenthesis ( ), whereas the units of the parameter are in brackets [ ]. When no dimensions are given, the parameter is to be considered dimensionless [1].

1. Air mass flow rate ($\dot{m}_{air}$) [lbm/sec].
2. Fuel mass flow rate ($\dot{m}_{fuel}$) [lbm/hr].

3. Adiabatic compressor efficiency (η_c).

4. Adiabatic gas generator turbine efficiency (η_{ggt}) and adiabatic power turbine efficiency (η_{pt}).

5. Brake specific fuel consumption (BSFC) $[\frac{lbm/hr}{SHP}]$.

6. Output shaft horsepower (SHP) and power turbine work (W_{PT}) [hp].

7. Gearbox efficiency (η_g).

8. Fuel to air ratio (f).

9. Thermal efficiency (η_{th}).

10. Compressor work (W_c) [hp].

11. Gas generator turbine work (W_{ggt}) [hp].

1. Air Mass Flow Rate

The measurement of the air flowing into the gas turbine engine is necessary for computation of total work of each engine component. In general the mass flow rate of air is not measured, but rather the volumetric flow rate (Q_{air}) is. From this volumetric flow rate, the mass flow rate of the air is determined from:

$$\dot{m}_{air} = \rho\, Q_{air} \tag{3.1}$$

The symbol "ρ" is the density of the air in pounds mass per cubic foot.

2. Fuel Mass Flow Rate

The mass flow rate of fuel ($\dot{m}_{fuel}$) entering the engine is used extensively in performance computations and requires measurement. The method of obtaining the fuel mass flow rate is discussed in Chapter IV.

3. Adiabatic Compressor Efficiency

The engine's two separate compressors are staged in series. Ideally, efficiencies should be calculated for each compressor. The equation for the adiabatic efficiency of the compressor (η_c) is shown in Equation 3.2; where π_c and τ_c represent the total pressure and total temperature ratios, respectively. The symbol γ is the specific heat ratio.

$$\eta_c = \frac{\pi_c^{\frac{\gamma-1}{\gamma}} - 1}{\tau_c - 1} \tag{3.2}$$

4. Gas Generator Turbine And Power Turbine Adiabatic Efficiencies

The adiabatic efficiency equation for both the gas generator turbine adiabatic efficiency (η_{ggt}) and the power turbine adiabatic efficiency (η_{pt}) are given by:

$$\eta_{ggt} = \frac{1 - \tau_{ggt}}{1 - \pi_{ggt}^{\frac{\gamma-1}{\gamma}}} \tag{3.3a}$$

$$\eta_{pt} = \frac{1-\tau_{pt}}{1-\pi_{pt}^{\frac{\gamma-1}{\gamma}}} \tag{3.3b}$$

Although the equations are identical, the computation of the pressure ratios are slightly different. In the gas generator adiabatic efficiency equation, the pressure ratio (π_{ggt}) is the ratio of total pressures. In the power turbine adiabatic efficiency equation, the pressure ratio (π_{pt}) is a ratio of static pressure to total pressure. Both definitions are commonly used. The reasoning behind measuring the static to total pressure ratio for the power turbine is that the use of any velocity component contained in the outlet total pressure of the power turbine is "wasted energy" since no additional work is done by the engine. This allows the engineer to establish how much work is extracted by the power turbine compared to the maximum amount of work that could be extracted if the combustion gases were expanded to ambient pressure with no exit kinetic energy.

5. Brake Specific Fuel Consumption

The *brake specific fuel consumption* (BSFC) is the ratio of the mass flow rate of fuel to the output shaft horsepower. The formula is seen in Equation 3.4.

$$BSFC = \frac{\dot{m}_f}{SHP} \tag{3.4}$$

6. Shaft Horsepower

Two methods are used in determining shaft horsepower of the gas turbine engine. The first uses a simple calculation of shaft torque (τ) multiplied by shaft speed (ω) in

revolutions per second as seen in Equation 3.5. The shaft horsepower relationship is multiplied by a factor of 550 to convert the units from foot pounds force per second to horsepower.

$$SHP = 550\tau\omega \tag{3.5}$$

The second method determines an approximate shaft horsepower using the relationship for power turbine work. The power turbine work measures the amount of energy taken directly from the combustion gases flowing through the power turbine. The amount of work done by the power turbine is given in Equation 3.6 and will be somewhat larger than the output shaft horsepower measured in Equation 3.5. Although the power turbine directly drives the output shaft, energy losses occur in the form of bearing friction, windage, and gear friction. Because of these frictional losses the work done by the power turbine will be slightly larger the actual horsepower measurement taken directly from the drive shaft. The power turbine work is a good *estimate* of the output shaft horsepower.

$$W_{PT} = 1.415(\dot{m}_{air} + \dot{m}_{fuel})c_p(T_{T5} - T_{T6}) \tag{3.6}$$

For Equation 3.6 the units of both mass flow rates are pounds mass per second and the temperatures are in degrees Fahrenheit. The units for heat capacity (cp) are BTU per pound mass degree Fahrenheit and a conversion factor of 1.415 converts these values to horsepower.

7. Gearbox Efficiency

The output shaft horsepower determined by the power turbine work is slightly larger than the shaft horsepower found using the torque- speed relationship. As discussed previously, this is due to mechanical energy losses throughout the reduction gear used to reduce the output shaft speed to 6,000 RPM. The ratio of these two power calculations defines the gearbox efficiency (η_g) as shown in Equation 3.7.

$$\eta_g = \frac{SHP}{W_{PT}} \tag{3.7}$$

8. Fuel - Air Ratio

The *fuel- air ratio* (*f*) is a given by the Equation 3.8. This ratio is unitless and care should be taken to ensure both mass flow rates are in identical units prior to computing this ratio.

$$f = \frac{\dot{m}_{fuel}}{\dot{m}_{air}} \tag{3.8}$$

9. Thermal Efficiency

For turboshaft engines, the *thermal efficiency* is defined as the ratio output shaft power to the total energy consumption rate $\dot{m}_{fuel}$ multiplied by Q_R, where Q_R is the lower heating value of the fuel. This simplified relationship is found in Equation 3.9. With the output shaft horsepower (SHP) in units of horsepower, the mass flow rate of fuel in units of pounds mass per hour, and the lower heating value of fuel in BTU per pound

mass, a conversion factor of 2544.43 is necessary to ensure the thermal efficiency is dimensionless.

$$\eta_{th} = 2544.43 \frac{SHP}{\dot{m}_{fuel} Q_R} \tag{3.9}$$

10. Compressor Work

Compressor work and the work of the gas generator turbine are roughly equal. The gas generator turbine work is slightly larger due to the fact that not only does it power the compressor, it also provides power to the pressure and scavenge oil pumps within the gearbox housing. The equations for compressor work and gas generator turbine work are given in Equation 3.10 and Equation 3.11, respectively. The work of both the compressor and the gas generator turbine are calculated in BTU per second. Both mass flow rates have the units of pounds mass per second. A conversion factor is again used to convert units to horsepower.

$$\dot{W}_{Comp} = 1.415 \dot{m}_{air} c_p (T_{T2} - T_{T1}) \tag{3.10}$$

$$\dot{W}_{GGT} = 1.415 (\dot{m}_{air} + \dot{m}_{fuel}) c_p (T_{T4} - T_{T5}) \tag{3.11}$$

B. UNCERTAINTY ANALYSIS

A certain degree of uncertainty surrounds the accuracy of the instruments used to measure any physical properties. When several different types of measuring instruments and their subsequent data are used in deriving mathematical expressions for engine

analysis, this degree of uncertainty is propagated. This section deals with the question of how accurate both temperature and pressure measurements must be in various components of the gas turbine engine in order to ensure a certain degree of accuracy in predicting component adiabatic efficiencies and hence, overall engine performance. The three major engine component efficiencies analyzed are:

1. Compressor
2. Gas Generator Turbine (GGT)
3. Power Turbine (PT)

The following is a list of assumption made for the analysis.

1. The specific heat ratio, γ, is constant between inlet and outlet conditions of each engine component. This value is found from averaging the thermodynamic predicted inlet and outlet temperatures and extracting it from the tables for dry air at one atmosphere.
2. The uncertainty in the pressure and temperature at the *inlet* to the compressor is negligible and can be omitted.
3. All uncertainty predictions are based on predicted thermodynamic cycle analysis and engine modeling data provided by Allison Division, Rolls Royce Corporation.

The most probable uncertainty in the component efficiencies is determined for the uncertainties in the pressure and temperature mèasurement made by use of the standard

methods [Ref. 2]. Appendix A contains the MATLAB m-file produced to obtain the uncertainty based on different temperature and pressure uncertainties.

Although the uncertainty analysis determines the requirements for instrument accuracy, it does not take into account irregularities in flow conditions throughout the engine. The uncertainty analysis assumes that the temperature and pressure sensing devices are already placed at the bulk averaged value of the physical property being measured. This is a very big assumption and one that can only be supported through experimentation with the measurement devices to find the correct placement within the flow. Because the pressure and temperature uncertainties of instrumentation equipment have the largest effect at low power conditions, the design requirements which are discussed in Chapter IV are based on the low power uncertainty analysis. For this reason, only low power uncertainty calculations are presented in this chapter.

1. Compressor Uncertainty

The adiabatic efficiency computed for this analysis incorporates both the axial and the centrifugal compressors as a single unit. The equation for the adiabatic efficiency of the compressor is shown in Equation 3.2. The uncertainty of the adiabatic compressor efficiency is found in Equation 3.12 shown below, where u_P and u_T are the uncertainty in the measurements of the outlet pressure and temperature.

$$U_{Comp} = \sqrt{(u_P \frac{\partial \eta_c}{\partial \pi_c})^2 + (u_T \frac{\partial \eta_c}{\partial \tau_c})^2} \tag{3.12}$$

Substituting the values for the partial derivatives of η_c the uncertainty for the compressor is shown below:

$$U_{Comp} = \sqrt{(u_P \frac{\gamma - 1}{\gamma} \frac{\pi_c^{\frac{\gamma-1}{\gamma}-1}}{\tau_c - 1})^2 + (u_T \frac{\pi_c^{\frac{\gamma-1}{\gamma}} - 1}{(\tau_c - 1)^2}} \quad (3.13)$$

Figure 3.2 displays the uncertainty in compressor efficiency at low power conditions with varying uncertainties in the temperature and pressure ratios. Looking at these figures, some general statements about the calculation of compressor efficiency can be made. First, the pressure ratio greatly influences the uncertainty of computed efficiency. For example, in the low power configuration for the engine, N1 at 85% of rated speed (Figure 3.1), a 10 °F error in the outlet temperature measurement contributes to roughly 2.2% uncertainty in computed efficiency. A 5 psi uncertainty in the outlet pressure measurement nearly doubles the amount of uncertainty in compressor efficiency to roughly 4.1% when compared to the temperature error. Second, the accuracy of compressor efficiency increases as N1 speed increases. The reason for this is due to the fact that as engine speed increases, so does the temperature and pressure ratio. This in turn decreases the effects of pressure and temperature ratio errors have on the overall uncertainty. This is readily apparent when looking at the maximum compressor uncertainty at the two different power settings shown for the engine. In the low power case (Figure 3.2) the maximum error is 5.5%, whereas in the high power case of N1 speed of 105%, Figure 3.3, the uncertainty drops to 2.75%.

2. Power Turbine and Gas Generator Turbine Uncertainties

The uncertainty of both the power turbine and gas generator turbine adiabatic efficiencies are similar to the compressor efficiency uncertainty analysis. The relationship for adiabatic efficiency of both turbines are shown in Equations 3.3a and 3.3b for the gas generator turbine and power turbine, respectively. Using the same analysis shown previously for the compressor, the uncertainties for the turbines become:

$$U_{PTorGGT} = \sqrt{\left[\frac{u_T^{\,2}}{(1-\pi^{\frac{\gamma-1}{\gamma}})^2}\right] + \frac{u_P(1-\tau)^2(\gamma-1)^2}{[(1-\pi)^{\frac{\gamma-1}{\gamma}}]^2\gamma^2(1-\pi)^2}} \qquad (3.14)$$

To avoid redundancy, the terms u_T, u_P, π, and τ in Equation 3.14 refer to the separate component's temperature and pressure uncertainties, as well as separate pressure and temperature ratios.

Figures 3.4 and 3.5 display the uncertainties calculated for the gas generator turbine and power turbine, respectively. As in the compressor analysis, the overriding factor in determining an accurate efficiency calculation is a precise measurement of pressure. The uncertainties for both the power turbine and the gas generator turbine efficiencies are much greater than that of the compressor efficiency uncertainty, due to the measurement errors recorded in both inlet and outlet conditions of each turbine. Unlike the compressor, where just the outlet conditions were assumed to have a large degree of uncertainty, both inlet and outlet conditions have appreciable errors present in the measurements taken. An odd situation arises in the uncertainty analysis of the power turbine at low speed (N1 = 85%). Figure 3.5 shows a possible uncertainty in efficiency

greater than 100%. This is caused by the uncertainty in the pressure ratio becoming much greater than unity. In reality, an uncertainty of greater than unity is impossible, however, the computer program used to calculate the uncertainty had prescribed error ranges and therefore computed these erroneous values.

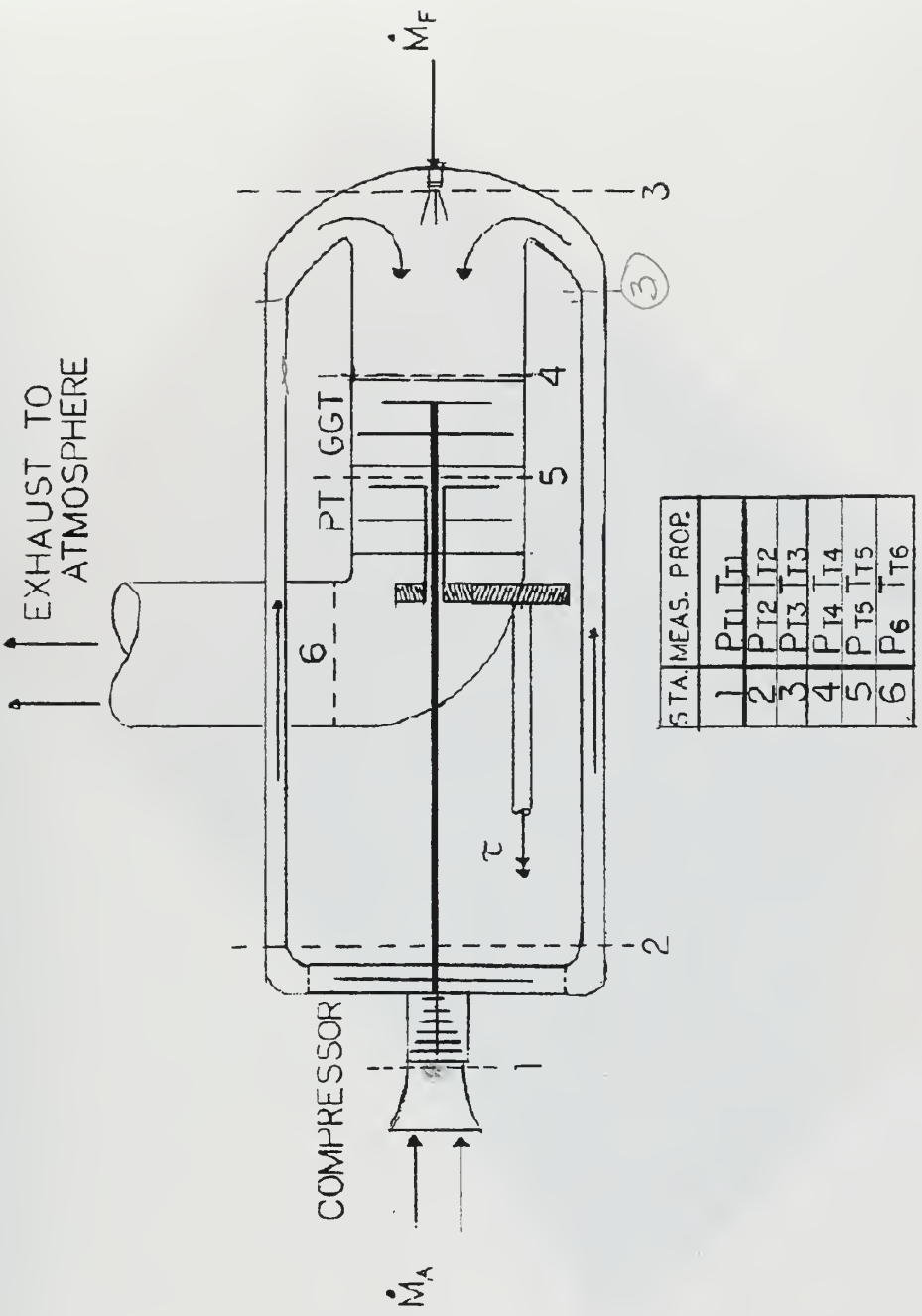

Figure 3.1. Schematic diagram of engine with state points.

Figure 3.2. Compressor low power uncertainty analysis plot.

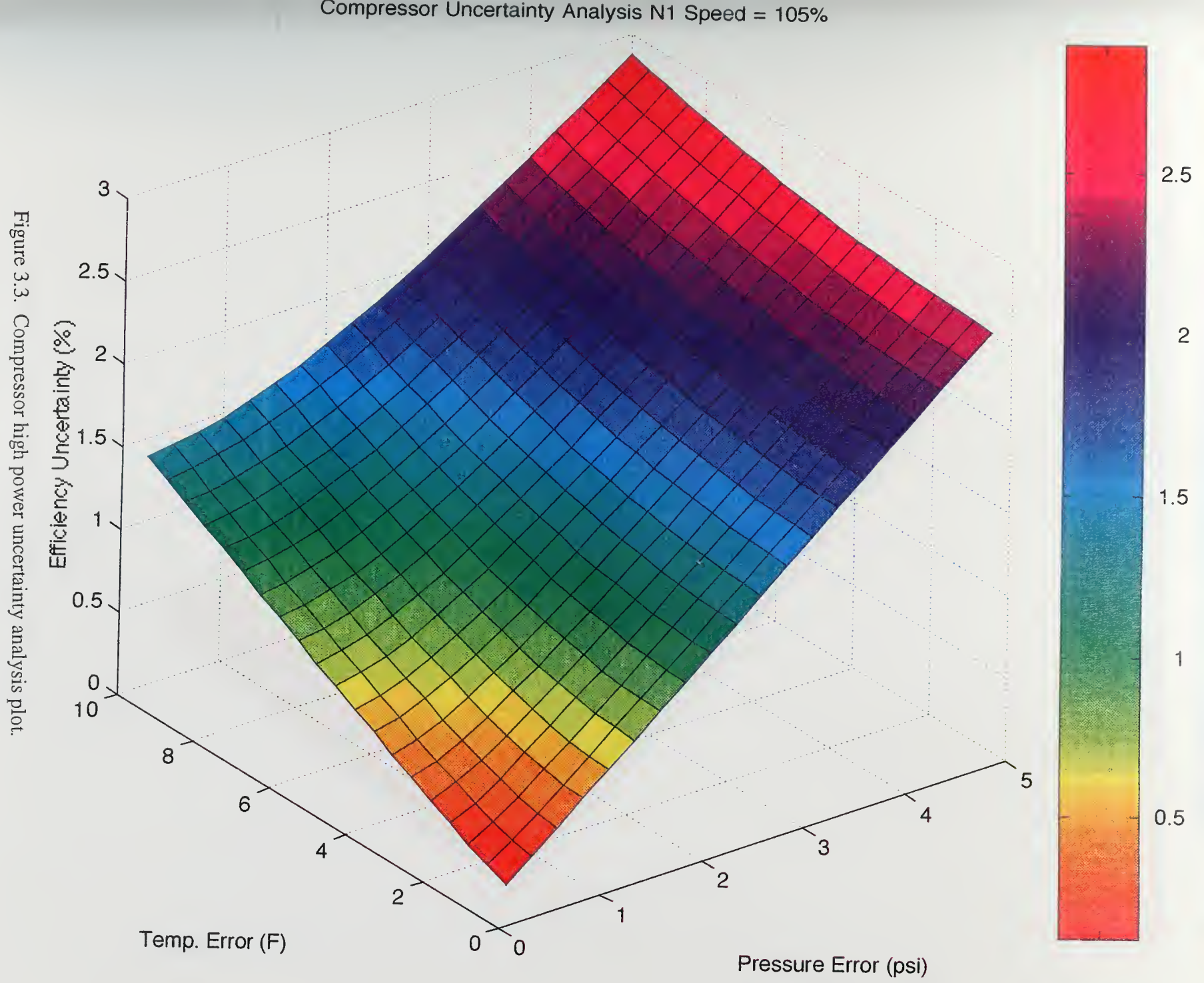

Figure 3.3. Compressor high power uncertainty analysis plot.

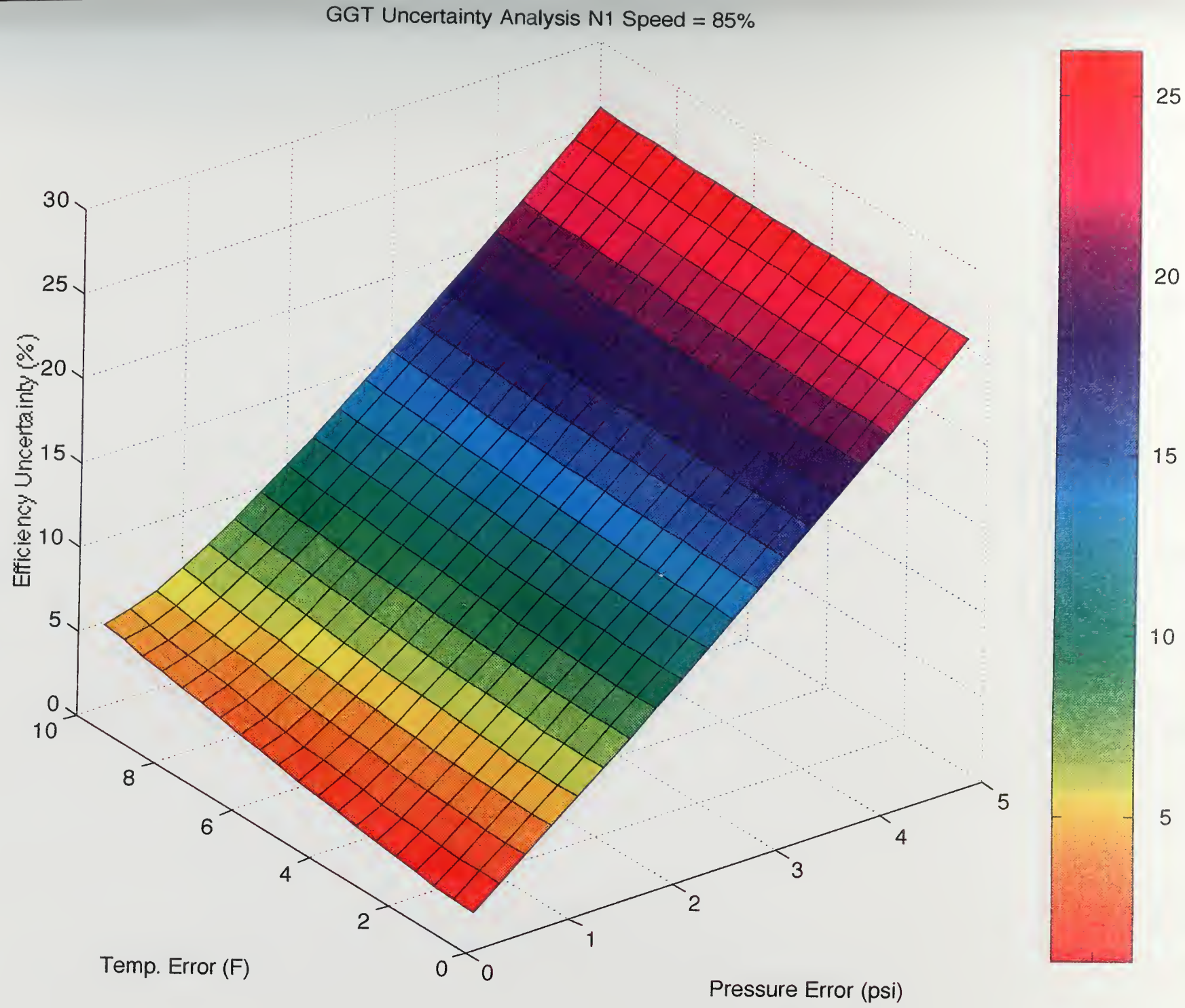

Figure 3.4. GGT low power uncertainty analysis plot.

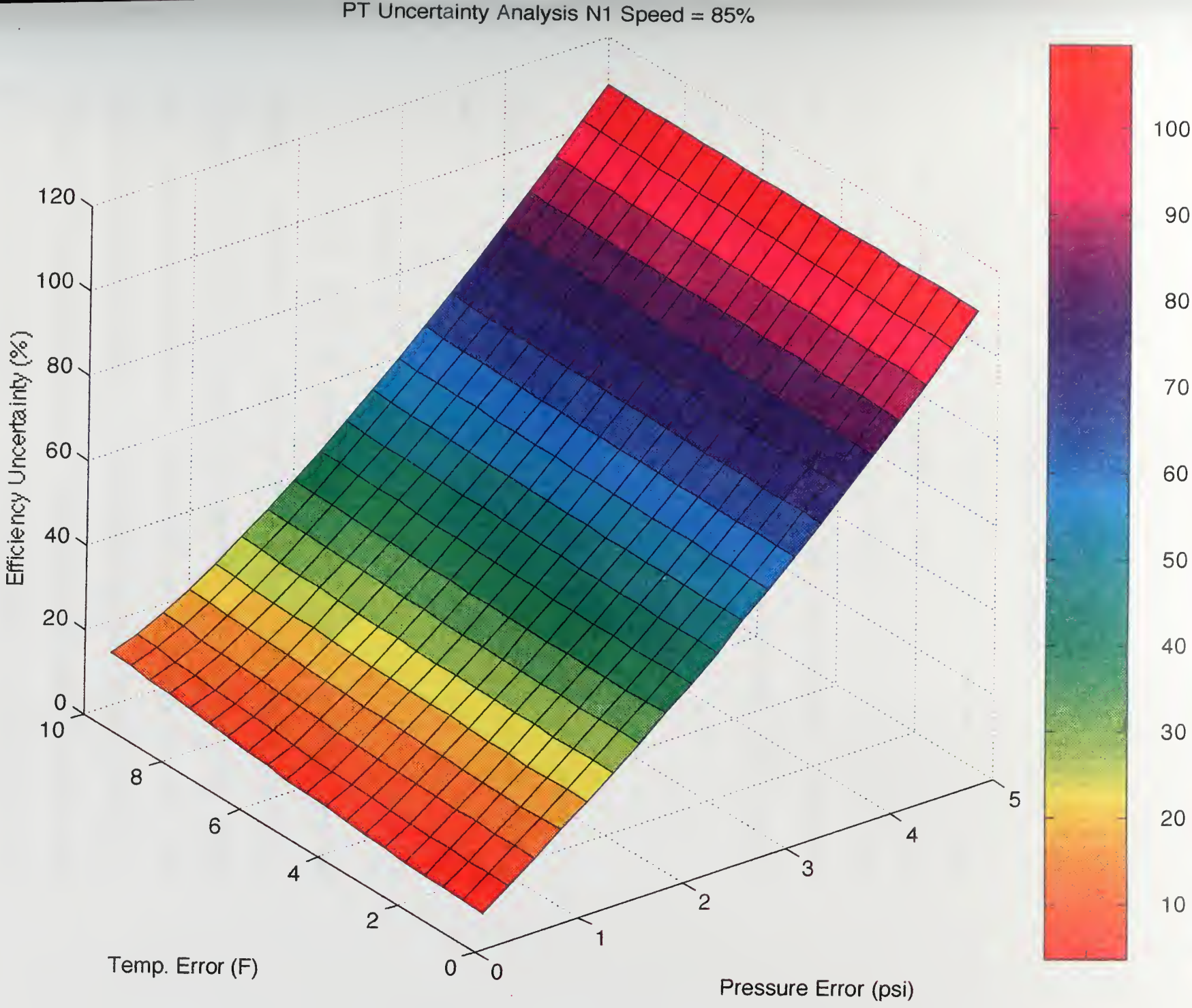

Figure 3.5. PT low power uncertainty analysis plot.

IV. INSTRUMENTATION DESIGN

In designing the instrumentation system for the gas turbine engine, the ultimate goal was to devise a measurement system to meet the requirements as presented in Chapter III. To do this, accurate measurement of the mass flow rate of air, the mass flow rate of fuel, temperature, and pressure throughout the engine was needed. This chapters discusses the design, fabrication, and installation of the measurement devices devised to meet these requirements.

A. DESIGN OBJECTIVES

There are five primary design requirements of the instrumentation system. The system must be accurate, safe, robust, easily installed and maintained, and simple to monitor.

1. Accuracy

In order to ensure the accuracy of the instrumentation package, component efficiency uncertainties of no more than 3% is desired. The required pressure and temperature sensitivities are obtained for the compressor, gas generator turbine, and the power turbine from the uncertainty analysis presented in Chapter III. For a 3% uncertainty in compressor efficiency, a corresponding temperature and pressure error of 2 °F and 2.75 psi, respectively, is required. For the gas generator turbine the corresponding pressure and temperature errors are 2 °F and 0.5 psi. Finally, for the power turbine the feasibility of a 3% uncertainty in the efficiency is unrealistic due to the requirement of

minute errors in both temperature and pressure. A more realistic efficiency uncertainty for the power turbine is 4.5%. With this uncertainty in efficiency, the pressure and temperature errors are 0.25 psi and 1 °F, respectively. The values for maximum errors and the corresponding efficiency uncertainty are found in Table 4.1.

2. Safety

Safety of personnel and the engine are primary concerns. Safety of personnel is accomplished through the use of Standard Operations Procedures and is discussed in Chapter VI. Safe operation of the engine and its instrumentation is accomplished through analytical modeling of measurement instruments to ensure failure from over stress conditions does not occur during all engine operating levels. Second, the design of instrumentation must maintain, as much as possible, the original integrity of the engine core as produced by the manufacturer in order to decreases the risk of catastrophic failure of the engine.

3. Longevity

In the design of instruments the use of proper materials, as well as proper placement, ensure a long life for each measurement device.

4. Ease of Installation and Maintenance

To ensure the continued accuracy of data, the instrumentation must be fairly easy to install and maintain. The design of the instrumentation package for the T63-A-700

engine ensures challenging but workable fabrication of instrumentation devices and a simple and easy means to install and maintain the instruments on the engine.

5. Instrumentation Monitoring

The monitoring of the installed instrumentation is accomplished through the use of computers. This allows rapid data acquisition and easy recording. The post processing of this data is accomplished again with a computer. The use of the computer for acquisition and post processing is further discussed in Chapter VI.

B. INSTRUMENTATION CONCERNS AND GENERAL DISCUSSION

To obtain the objectives discussed in Chapter III a single pressure and temperature reading for each state point shown in Figure 3.1 is required. For an accurate measurement these values must be the "bulk average" values. Obtaining this "bulk average" is a challenge due to the possibility of unsteady and non-uniform flow conditions. Additionally, throughout the engine the exact direction of the flow is unknown. Another concern for instrumentation is the feasibility to access some engine components for monitoring. This requirement to monitor certain points throughout the engine must be weighed against two of the primary design objectives of safety of the engine and ease of installation.

A final point of discussion deals with the measurement of total versus static pressure and temperature and the need to measure one or the other throughout the engine. A close approximation of total temperature is obtained when placing a temperature measurement device in the flow path of the working fluid. Because all temperature

devices in the engine are placed in the flow path of the air, total temperatures are collected and are used for engine behavior and performance calculation. Deciding which type of pressure measurement to monitor, however, is not quite as simple.

The flow patterns at the exits of the major engine components (compressor, gas generator turbine, and power turbine) are extremely difficult to predict analytically. In general, direction of the flow will be axial as the air flows from a high pressure region to a low pressure region from component to component. However, the possibility for swirl of the flow in any direction is very likely to occur throughout the engine. The swirl of the flow can cause an inaccurate reading of a static pressure measurement. With an inaccurate static pressure measurement, the total pressure derived from the static pressure measurement will also be in error. Therefore, inaccurate calculations of engine performance will be computed. For this reason the use of static pressure measurement at the casing in the computation of engine behavior and performance is discouraged. The total pressure measurement, therefore, is used to compute the objectives stated in Chapter III except where a static measurement is required as stated.

Working within the parameters of the design objectives, and taking these instrumentation concerns and comments under consideration, an instrumentation package has been designed, fabricated and installed on the gas turbine test cell. The ensuing discussion details the measurement instruments in use on the engine.

C. MEASUREMENT DEVICES AND LOCATIONS

Figure 3.1 contains the schematic diagram for the Marine Propulsion Laboratory gas turbine engine. This section discusses the different types of measuring devices used throughout the engine to measure temperature, pressure, and mass flow of fuel and air.

1. Mass Flow Rate Measurement Devices

Volumetric flow rates of air and fuel are measured and a mass flow rate is then derived from a density correction factor based on temperature. Air flowing to the engine is measured twice. First, dual turbine flowmeters are installed on the engine's inlet plenum as shown in Figure 4.1. From this volumetric flow rate of air, the mass flow rate is then calculated based on inlet temperature conditions. The Superflow 901 system displays the volumetric flow rate in cubic feet per minute (CFM). Second, a calibrated bell mouth is placed on the compressor inlet. Knowing the cross-sectional area of the bell mouth housing and the total pressure at the compressor inlet, the mass flow rate of the air is computed.

The measurement of fuel flow is also accomplished through the use of a turbine flowmeter. Once again the mass flow rate is derived from the volumetric flow rate. The specific gravity of the fuel is corrected based on temperature conditions. The engine operator inputs the measured specific gravity of the fuel into the Superflow 901 system, which then computes the mass flow rate of the fuel in pounds mass per hour.

2. Pressure Measurement Devices

To measure total pressures throughout the engine, both Pitot tubes and Kiel-type probes have been selected. Additionally, the measurement of static pressure where necessary is accomplished through the use of static pressure rings. Both Kiel probes and Pitot tubes are point specific measurements. This means that either pressure sensing device gives the pressure at a certain point in the flow. For this reason, proper location is necessary in a non-uniform flow. Experimentation must be conducted to find the pressure profile at each state point monitored in the engine, and the probes placed at the average value. This is sometimes difficult to accomplished and assumptions must be made.

The primary concern in using the Pitot tube for the measurement of total pressure is ensuring that the probe is aligned with the incoming flow direction. Because the Pitot tube is somewhat sensitive to flow alignment, a large misalignment (5°) of the probe axis with the flow pattern decreases the accuracy of the total pressure measurement. The angle formed between the probe axis and the flow streamline at the pressure opening is called the *yaw angle*. Ideally this angle should be zero. The errors incurred are shown in Figure 4.2. The advantage of a Pitot tube over a Kiel probe, however, is the Pitot tube in general is far easier to fabricate than a Kiel probe and is less costly.

The Kiel probe is also designed to measure total pressure. It consists of a Pitot tube surrounded by a tube which aligns the flow normal to the Pitot inlet. Figure 4.3 demonstrates the insensitivity to variation in the yaw angle found with a Kiel probe. The insensitivity to flow direction found in the Kiel probe is an advantage when some swirl is present and hence the direction of the flow is unpredictable. Figure 4.4(a) and Figure

4.4(b) show the two types of Kiel probes installed as part of the instrumentation package. Figure 4.4(b) is a combination Kiel probe - thermocouple device used to measure both total temperature and pressure.

a. Compressor Inlet (P_{T1})

Located in the bell mouth housing are two types of pressure measurements devices. First, a single Pitot tube measures the total pressure (P_{T1}) entering the compressor. With the air flow rapidly accelerating in the compressor the assumption of a "slug-like" velocity profile of the flow is reasonable, allowing the use of this point measurement device to represent the pressure characteristics of the flow. Additionally, this rapid acceleration ensures a truly axial flow path and allows the Pitot tube to read the true total pressure. A static pressure ring has been placed on the inner surface of the bell mouth with four inputs that are mechanically averaged. This measurement of both static and total pressure combined with the knowledge of the cross-sectional area of the bell mouth allow a good comparison between the air flow rate measured by the turbine flowmeters with that of the flow rate found from the static and total pressure difference.

b. Compressor Outlet (P_{T2})

The compressor outlet temperature is measured using the Kiel-type probe found in Figure 4.4(b). An exploded view of the probe is shown in Figure 4.5 and an installed view is shown in Figure 4.6. The probes are placed between the exits of the scroll type diffuser and the inlet to the two circular ducts (Figure 2.1). At the exit of the compressor the mass flow of air is passing through the smallest cross sectional flow area

encountered within the engine. This small cross sectional area along with the high density consequently causes the highest Mach numbers found in the air flow path. At full power (N1 = 51,120 RPM) the Mach number at the discharge of the compressor is 0.38. Because of this high Mach number a complete stress analysis for both the dynamic and the static cases for the Kiel probes is discussed.

(1) Static Stress Analysis

The Kiel probes at the compressor discharge are modeled as cantilever beams with a uniformly distributed load. The engine presumably has been designed to evenly distribute the mass flow of air into each circular duct. Because of this even distribution of air, the analysis for each Kiel probe located at the compressor discharge is identical. The Kiel probes installed in the power turbine section are under much lower forces as seen by the low Mach numbers found in that section of the engine (roughly 0.05 at full power). An identical analysis for these probes is conducted later in this section.

The Kiel probe particulars for the probes located at the compressor discharge are given in Table 4.2. The air parameters at full power (N1 = 51,120 RPM) are given in Table 4.3.

From these parameters the Mach number and Reynolds number are calculated. From the Reynolds number a drag coefficient (C_D) is obtained. [Ref. 5: p. 272] Using the drag coefficient, the drag force (F_D) is calculated. The relationship for the drag force is shown below:

$$F_D = \frac{1}{2} C_D \rho V^2 A \tag{4.1}$$

where A is the cross-sectional area normal to the flow. The tabulated values for the Mach number, Reynolds number, drag coefficient, and drag force are found in Table 4.4.

By dividing the drag force by the length of the probe, the force per unit length of the uniform load is obtained. The maximum moment on the probe is found using the relationship in Equation 4.2.

$$M_{max} = \frac{f_d L^2}{2} \tag{4.2}$$

Having found the maximum moment in the probe, the maximum bending stress is computed from the relationship displayed below:

$$\sigma_{max} = \frac{M_{max} R}{\frac{\pi}{4}(R^4 - r^4)} \tag{4.3}$$

This bending stress is then compared to the yield stress for 304 stainless steel and a factor of safety is determined. The maximum moment, maximum bending stress, yield stress, and the factor of safety are found in Table 4.5. The overall static stress safety factor is 6.33.

The data in Table 4.5 indicate that the static loading of the Kiel probe located at the compressor discharge will not cause failure under the most extreme static conditions in the engine.

(2) Dynamic Stress Analysis

The probe support will experience a dynamic force in the direction transverse to the main flow due to vortex shedding. If the vortex shedding frequency of the probe (and hence the forcing frequency) is near that of a natural frequency, resonance occurs and the probe may fail in high cycle fatigue. The failure of a probe at this point would allow metal matter to flow into the gas generator turbine, causing a catastrophic failure of the engine. For this reason the design of the Kiel probe must ensure the vortex shedding frequency and the natural frequencies of the probe are substantially different.

The vortex shedding frequency is determined experimentally and is proportional to the Strouhal number (*St*). The relationship for the vortex shedding frequency is given by Equation 4.4.

$$f_v = \frac{StV}{D_{eff}} \tag{4.4}$$

Experimental results show that the Strouhal number is relatively constant for Reynolds numbers between 10^4 and 10^5. The value of the Strouhal number at this Reynolds number is approximately 0.2. [Ref. 5: p. 270] Using the data found in Table 4.2 and Table 4.3 the vortex shedding frequency is found to be 10.96 Khz and is shown in Table 4.6.

The natural frequencies of the probe are based on the model of a cantilever beam. The first and second natural frequencies [Ref. 6. p: 226] are, respectively:

$$f_{n1} = \frac{1.875^2}{2\pi}\sqrt{\frac{EI}{mL^4}} \tag{4.5}$$

$$f_{n2} = \frac{4.694^2}{2\pi}\sqrt{\frac{EI}{mL^4}} \tag{4.6}$$

E is the Modulus of Elasticity. I is the moment of inertia. The mass per unit length is given as m. Finally, L is the length of the probe in the air flow.

The two natural frequencies found in Table 4.6 correspond to two different air velocities. For the first natural frequency (2.94 Khz) the velocity is 137.5 feet per second. This velocity in turn corresponds to an engine speed which is well below any operating velocity experienced in the engine. During start and shutdown a velocity will be reached where the shedding frequency sweeps through the natural frequency but will pass quickly, causing no damage to the probe or engine. The second natural frequency of the Kiel probe (16.5 Khz) corresponds to a velocity of 859.4 feet per second. At no time does the velocity of the air reach such a speed at the discharge of the compressor. Hence, this natural mode is not a problem.

(3) Fatigue

The final stress analysis deals directly with fatigue and life of the probe. Because the probe is made from 304 stainless steel there is no point on an S-N curve where infinite life of the probe is achieved, due to stainless steel's FCC crystal lattice structure. The amplitude of the vortex shedding force is thus important to find; because this problem is extremely complex and must be determined experimentally, a reasonable assumption must be made. It can be shown that the amplitude of the vortex shedding force will not exceed that of the maximum static force and thus the stress. Using

the maximum static stress of 6.32 kpsi as the amplitude of the cyclic stress and entering an S-N diagram for 304 stainless steel the cyclic life of the probe exceeds 10^{11} cycles which corresponds to 21.57 operating years of life for the probe under theses conditions. Therefore, fatigue of the probe is not a concern.

c. Combustor Inlet (PT3)

The measurement of pressure is not accomplished at the inlet to the combustor due to the thickness of the combustor casing being too thin to safely install a pressure measurement device.

d. Gas Generator Turbine Inlet (P_{T4})

The total pressure measurement for the inlet of the gas generator turbine is accomplished by two Pitot tubes located on the thermocouple ring assembly in Figure 4.7. These Pitot tubes are made from Inconnel 600 and are 1/8" in diameter and placed 180° apart from each other. These two pressure measurements are individually read by the monitoring system and averaged to obtain a single value for P_{T4}.

e. Power Turbine Inlet (P_{T5})

Figure 4.4(a) displays the Kiel probe design used in measuring the gas generator outlet pressure (P_{T5}). These Kiel probes are inserted through two of the existing openings for the onboard engine thermocouple harness. By inserting the probes through the harness the integrity of the engine casing is maintained. The two probes are located 90° apart from each other and are place at the midpoint of the flow path as shown in

Figure 4.8. Figure 4.9 shows the actual probe and its support structure while Figure 4.10 show the probes placed within the engine along with the thermocouple harness. Each pressure is taken separately then both are averaged to obtain an overall average total pressure. Because the Mach number at the power turbine inlet is very low (M = 0.05) stresses in excess of failure criteria are not expected and no stress analysis was conducted.

f. Power Turbine Exhaust (P_6)

A static pressure measurement is taken at the exhaust of the power turbine as an industry standard. This is accomplished on this engine by the use of a static pressure ring located on each exhaust pipe. Each ring consists of 8 static pressure points that are mechanically averaged. Each static pressure is individually read by the monitoring system; the values are then averaged to achieve a single exhaust pressure.

3. Temperature Measurement Devices

The measurement of temperature throughout the engine is accomplished by using K-type thermocouples. The K-type thermocouple has been selected due to its large operating range (0 - 2,500 °F) and its accuracy. Thermocouples are placed at both the inlet and outlet of each major component of the engine to include: the compressor, the gas generator turbine, and the power turbine.

a. Compressor Inlet (T_{T1})

The compressor inlet total temperature (T_{T1}) is measured using two K-type thermocouples. These are placed within the calibrated bell mouth housing at two different radii. The measurement temperatures are then averaged.

b. Compressor Outlet (T_{T2})

The outlet total temperature of the compressor is measured by two thermocouples that have been placed within the Kiel probe (Figure 4.4(b)). These two temperatures are also averaged to compute a single final compressor discharge temperature (T_{T2}). Figure 4.5 pictures the actual Kiel - thermocouple probe installed, while Figure 4.6 pictures the probe installed within the compressor discharge flow path.

c. Combustor Inlet (T_{T3})

To maintain engine integrity for reasons of safety the measurement of the air entering the combustor is not accomplished in the instrumentation package. It is expected, however, that there will be a drop in temperature from the compressor discharge to the combustor inlet due to losses in the circular ducts from the compressor to the combustor. These losses do not affect the computation of efficiencies, but will affect the thermodynamic calculation of gas generator inlet temperature (T_{T4}). This is discussed in Chapter VI.

d. Gas Generator Turbine Inlet (T_{T4})

The accurate temperature measurement of the hot combustion gases entering the gas generator turbine is a challenge, due to the possibility of a large non-uniformity in fuel burn. Because of the non-uniformity of combustion, a wide variety of temperature ranges may be observed entering the gas generator turbine. To overcome this problem, a large number of temperature measurements are made to give a more accurate averaged value of the inlet temperature (T_{T4}).

A thermocouple ring of 48 K-type thermocouples is placed at the entrance of the gas generator turbine. Figure 4.7 shows a drawing of the thermocouple ring assembly. The thermocouples are placed 7.5° apart and are placed radially at three different radii with sixteen at each radius.

The thermocouple wires are surrounded by a 1/16" Inconnel sheath designed for protection of the alumel and chromel wires in areas of extremely high temperatures. The ring assembly is fabricated out of 347 stainless steel, utilizing the high strength characteristics of this steel at high temperatures. The thermocouples are fitted in between the two pieces of the ring assembly as shown in Figure 4.11 to allow the changing of a thermocouple should it be damaged. The actual thermocouple ring assembly is shown in Figure 4.12 with a picture of the assembly installed in the engine in Figure 4.13.

To determine a true average temperature of the combustion gases entering the gas generator turbine (T_{T4}), a mass weighted technique is appropriate. The difficulty in using this technique is that a precise velocity profile of sufficient spatial resolution is required at

the gas generator turbine entrance. Below is the integral for determining the enthalpy per unit mass entering the gas generator turbine (Equation 4.7). This integral is the energy equation used in the mass weighted technique.

$$h_{ma} = \frac{\int (c_p T) d\dot{m}}{\int d\dot{m}} \tag{4.7}$$

The intergrand $d\dot{m}$ can be simplified into its components. Equation 4.8 shows the simplification of the intergrand.

$$h_{ma} = \frac{\int \int c_p T \rho (\vec{v} \bullet \hat{n}) r dr d\theta}{\int \int \rho (\vec{v} \bullet \hat{n}) r dr d\theta} \tag{4.8}$$

Having no way to determine the velocity profile entering the gas generator turbine an assumption is made that the flow of combustion gases is uniform and only in the normal direction (axial). This assumption is reasonable due to the large acceleration the combustion gases undergo prior to entering the gas generator turbine. With this assumption and that of constant density, Equation 4.8 reduces to:

$$h_{ma} = \frac{\rho v \int \int c_p T r dr d\theta}{\rho v \int \int r dr d\theta} \tag{4.9}$$

By using numerical techniques for the temperature value in the integral, the equation of area averaged enthalpy can be reduced further to:

$$h_{ma} = \frac{[c_p T_{thermo,in}(r_1^2 - r_{root}^2)] + [c_p T_{thermo,mid}(r_2^2 - r_1^2)] + [c_p T_{thermo,out}(r_{tip}^2 - r_2^2)]}{(r_{tip}^2 - r_{root}^2)} \tag{4.10}$$

The terms $T_{thermo,in}$, $T_{thermo,mid}$, and $T_{thermo,out}$ refer to the average temperature found from the thermocouple ring at each location - inner, middle, and outer radii, respectively, located on Figure 4.7. These three average temperatures are computed by simply averaging the sixteen temperature readings. The terms r_{root} and r_{tip} refer to the root and tip radii of 2.573" and 3.180", respectively, at the inlet to the gas generator turbine. Additionally, r_1 and r_2 are the radii found equidistant between thermocouples of 2.865" and 3.025", respectively.

Having solved for the area averaged enthalpy (h_{ma}), A single value for the gas generator inlet temperature is obtained by the relationship found in Equation 4.11. The specific heat value used is the average value derived from the three separate specific heat values used in Equation 4.10.

$$T_{T4} = \frac{h_{ma}}{c_p} \tag{4.11}$$

e. Power Turbine Inlet (T_{T5})

The power turbine inlet temperature (T_{T5}) is also the gas generator outlet temperature. This temperature is computed using the onboard thermocouple harness installed on the T63-A-700 gas turbine engine. The onboard engine thermocouple harness has been modified from four K-type thermocouples located 90° apart to two thermocouples located in just two of the four possible quadrants. The two other locations for the original thermocouple harness were replaced by two Kiel probes for pressure

measurement. The thermocouples are internally wired in parallel and do not require any external averaging.

f. Power Turbine Exhaust (T_{T6})

The exhaust of the power turbine is split into two separate ducts. Each duct has been instrumented with two K-type thermocouples. These values are taken and averaged to determine a final power turbine outlet temperature (T_{T6}).

Engine Component	*Desired Efficiency Uncertainty [%]*	*Maximum Pressure Error Allowable [psi]*	*Maximum Temperature Error Allowable [°F]*
Compressor	3	2.75	2
Gas Generator Turbine	3	0.5	2
Power Turbine	4.5	0.25	1

Table 4.1. Uncertainty requirements at low power (N1 = 85%).

Probe Diameter (D) [in]	*Frontal Area of Stem (A_{stem}) [in^2]*	*Frontal Area of Head (A_{head}) [in^2]*	*Total frontal Area (A_{total}) [in^2]*	*Probe outside radius (R) [in]*	*Probe inside radius (r) [in]*
0.125	0.1484	0.00307	0.15147	0.0625	0.0425

Table 4.2. Compressor discharge Kiel-type probe particulars.

Velocity [f t/sec]	*Temp. [°F]*	*Area [in^2]*	*Pressure [psi]*	*Compressor Effective Diameter [in.]* $D_{eff} = (\frac{4A}{P})$	*Air Mass Flowrate [lbm/sec]* ($\dot{m}_{air}$)	*Kinimatic Viscosity [ft^2/sec]* (ν)	*Density [lbm/ft^3]* $\rho = (\frac{P}{RT})$
571	504	1.5625	90.40	1.25	3.14	4.54×10^{-4}	0.25335

Table 4.3. Air parameters for compressor discharge.

Mach Number	*Reynolds Number*	*Drag Coefficient (C_D)*	*Drag Force (F_D) [lbf]*
0.38	13,1011	1.2	1.6632

Table 4.4. List of tabulated values for 1/8" Kiel-type probe located at compressor discharge.

Maximum Moment (M_{max}) *[lbf-in]*	*Maximum bending stress* (σ_{max}) *[kpsi]*	*Yield Stress for 304 Stainless Steel* (σ_{yield}) *[kpsi]*	*Safety Factor* ($\sigma_{yield}/\sigma_{max}$)
0.95288	6.321	40.0	6.33

Table 4.5. Stress value calculation for 1/8" Kiel-type probe located at the compressor discharge.

Vortex Shedding Frequency (f_v) *[Khz]*	*1st Natural Frequency of Kiel Probe* (f_{n1}) *[Khz]*	*2nd Natural Frequency of Kiel Probe* (f_{n2}) *[Khz]*
10.96	2.64	16.5

Table 4.6. Tabulate frequency data for 1/8" Kiel-type probe.

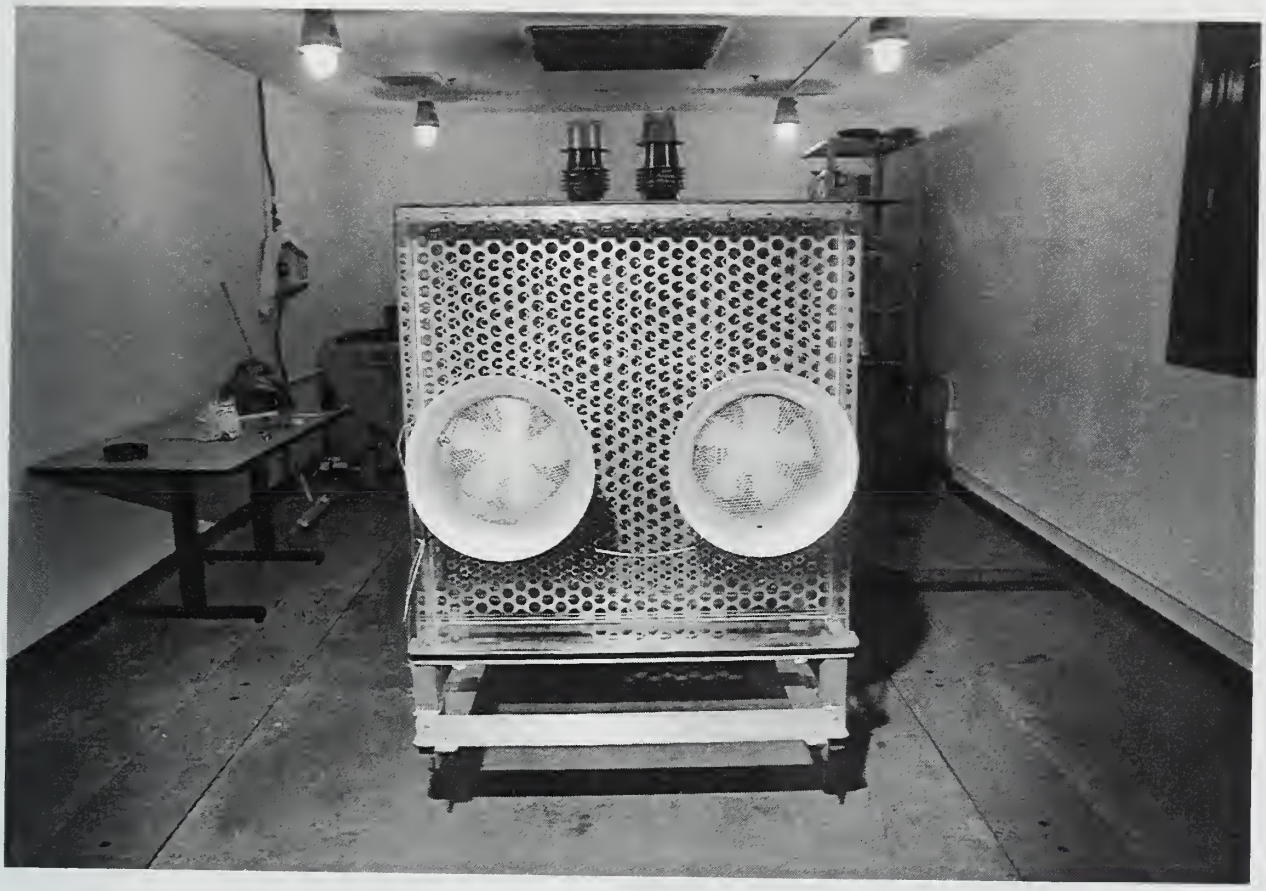

Figure 4.1. Dual air turbine flowmeters.

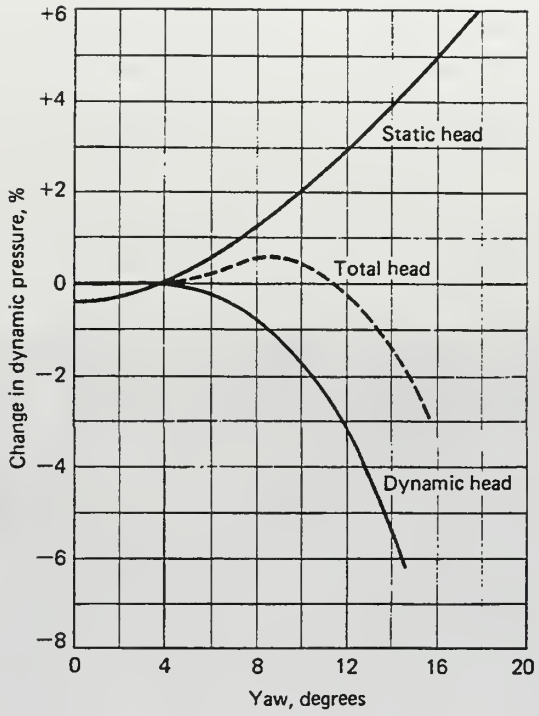

Figure 4.2. Yaw sensitivity of a standard Pitot tube. "From Ref. [3]"

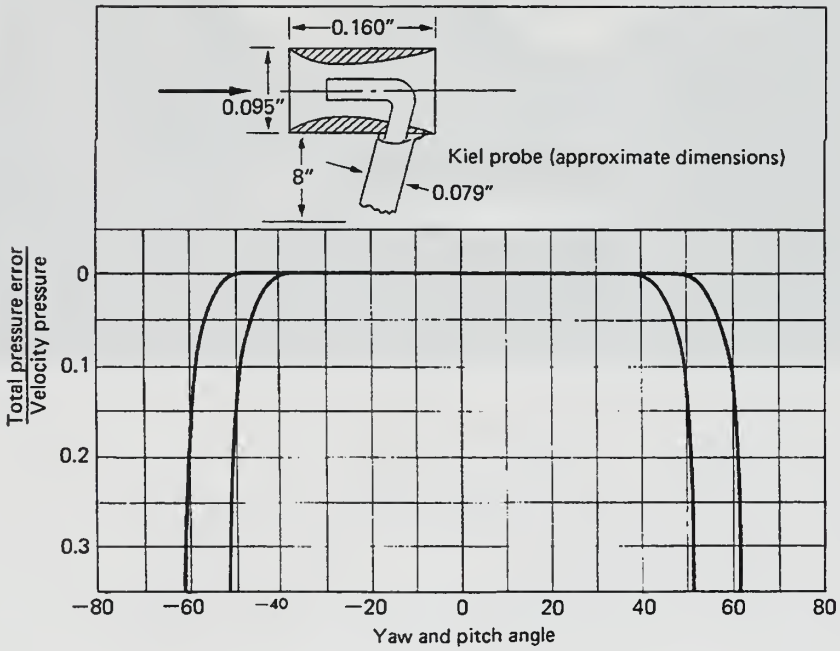

Figure 4.3. Kiel-type total pressure tube and plot of yaw sensitivity "From Ref. [3]."

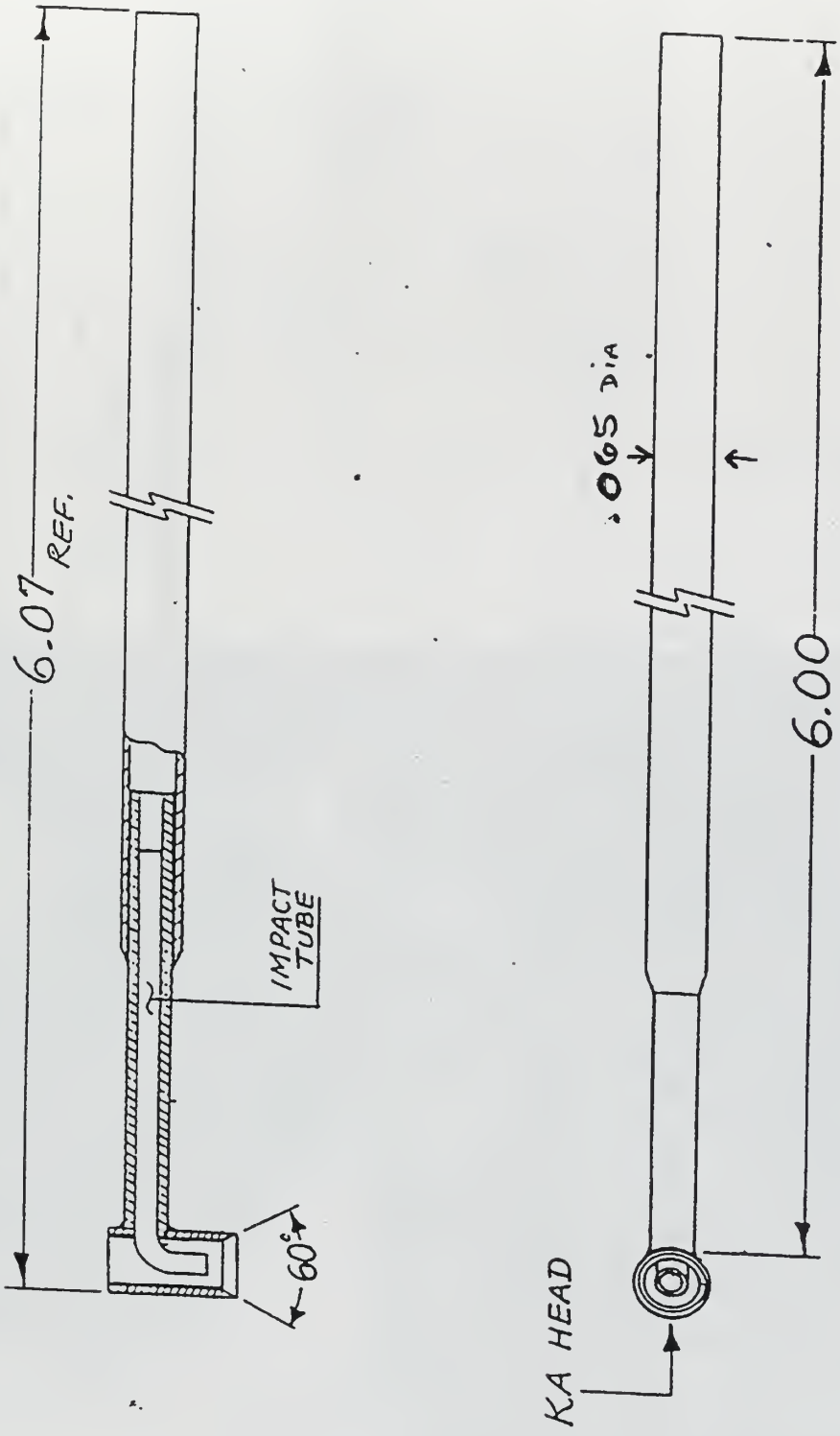

Figure 4.4(a). 1/16" Kiel probe used for total pressure measurement. "From Ref. [4] with permission from United Sensor Corp."

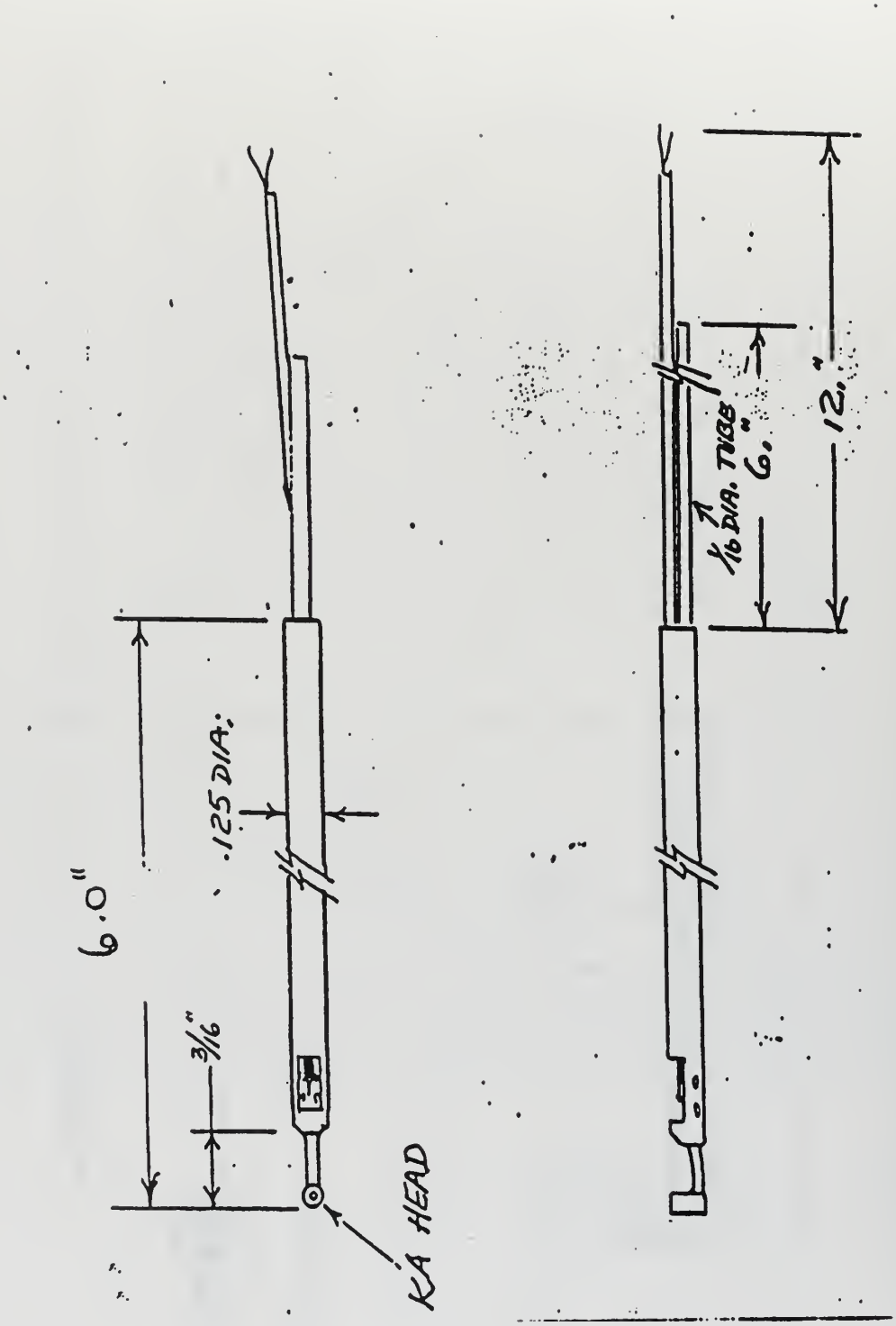

Figure 4.4(b). 1/8" combination Kiel - thermocouple probe. "From Ref. [4] with permission from United Sensor Corp."

Figure 4.5. 1/8" combination Kiel - thermocouple probe used for compressor discharge measurements.

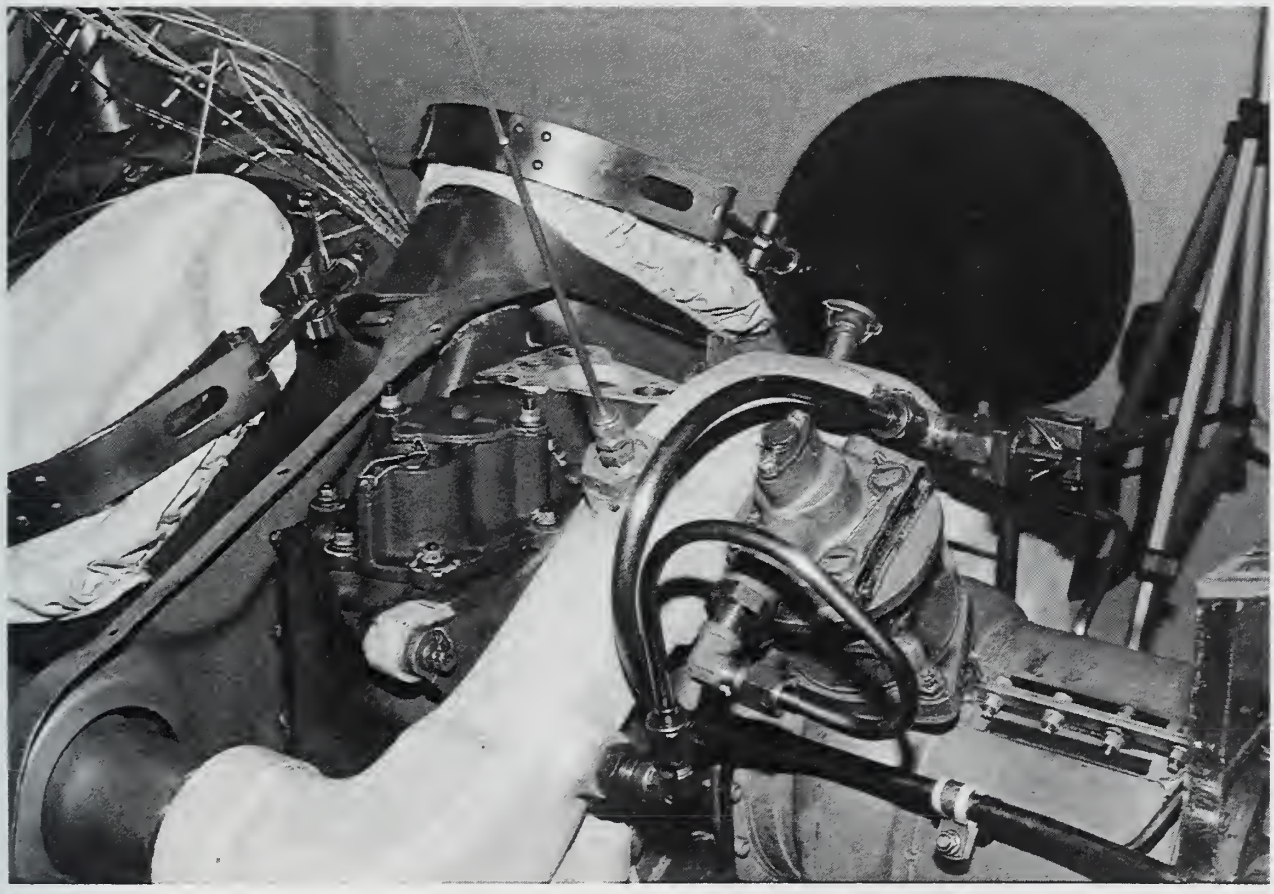

Figure 4.6. Installed view of Kiel - thermocouple probe on compressor discharge.

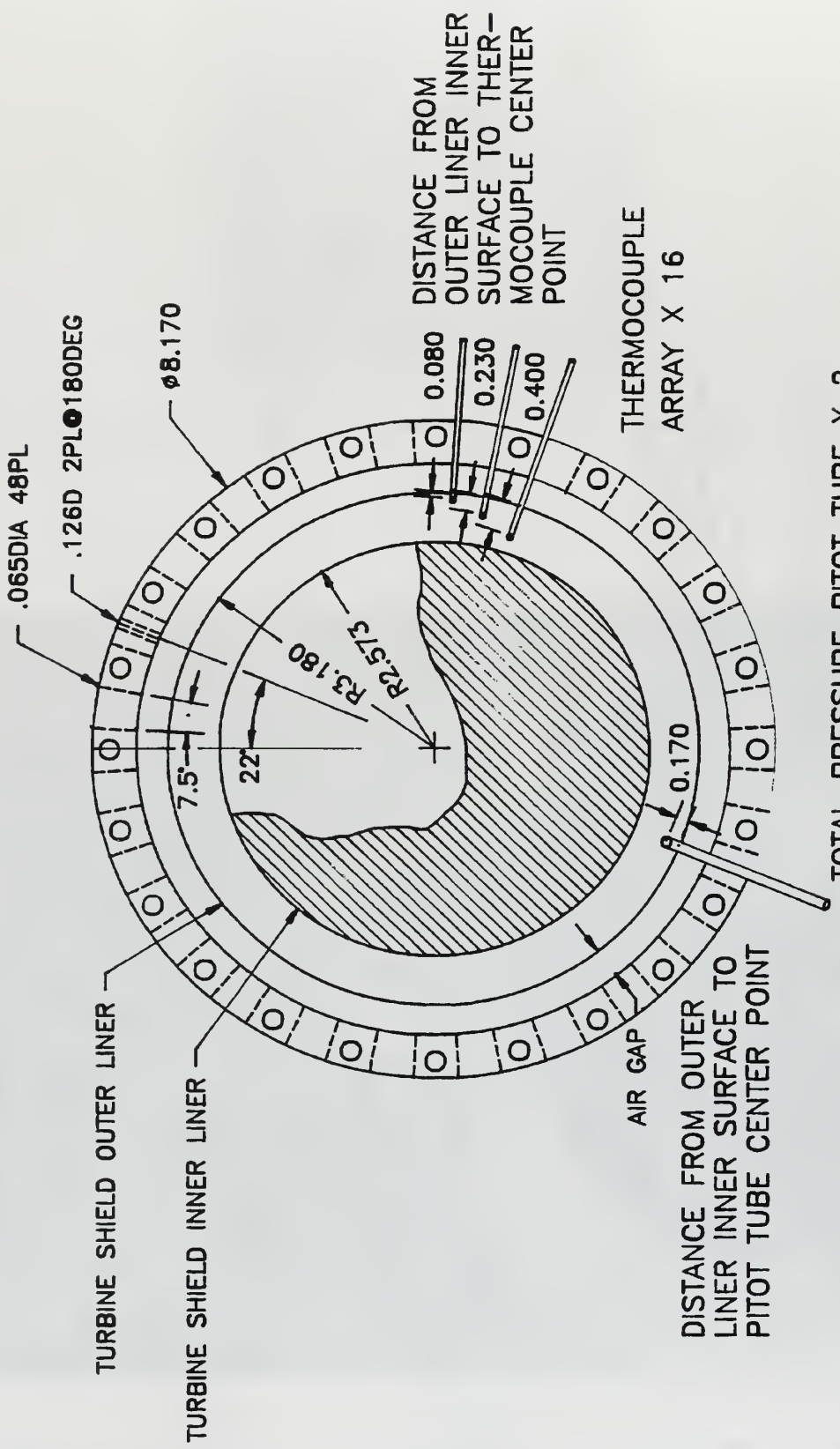

Figure 4.7. Drawing of GGT ring assembly.

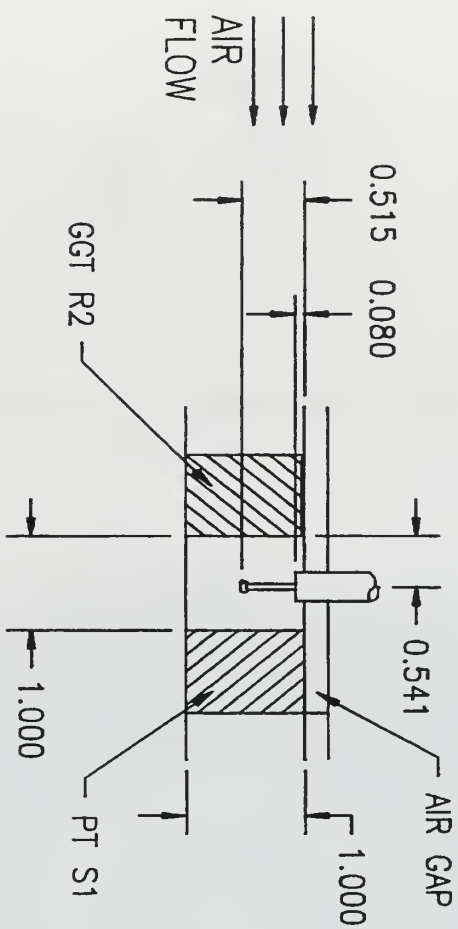

Figure 4.8. Power turbine Kiel probe placement.

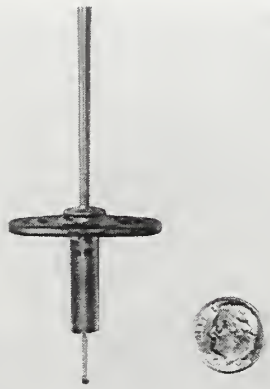

Figure 4.9. Power turbine Kiel probe and support structure.

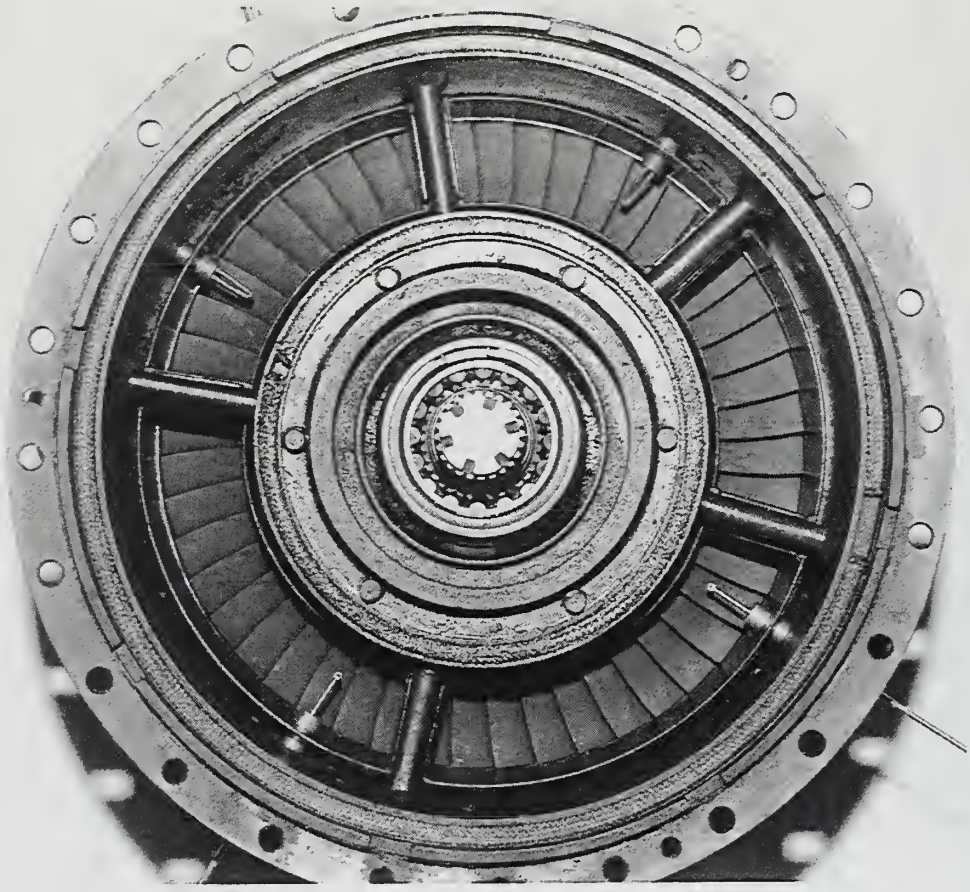

Figure 4.10. Installed view of both Kiel probes and thermocouples for the power turbine inlet conditions.

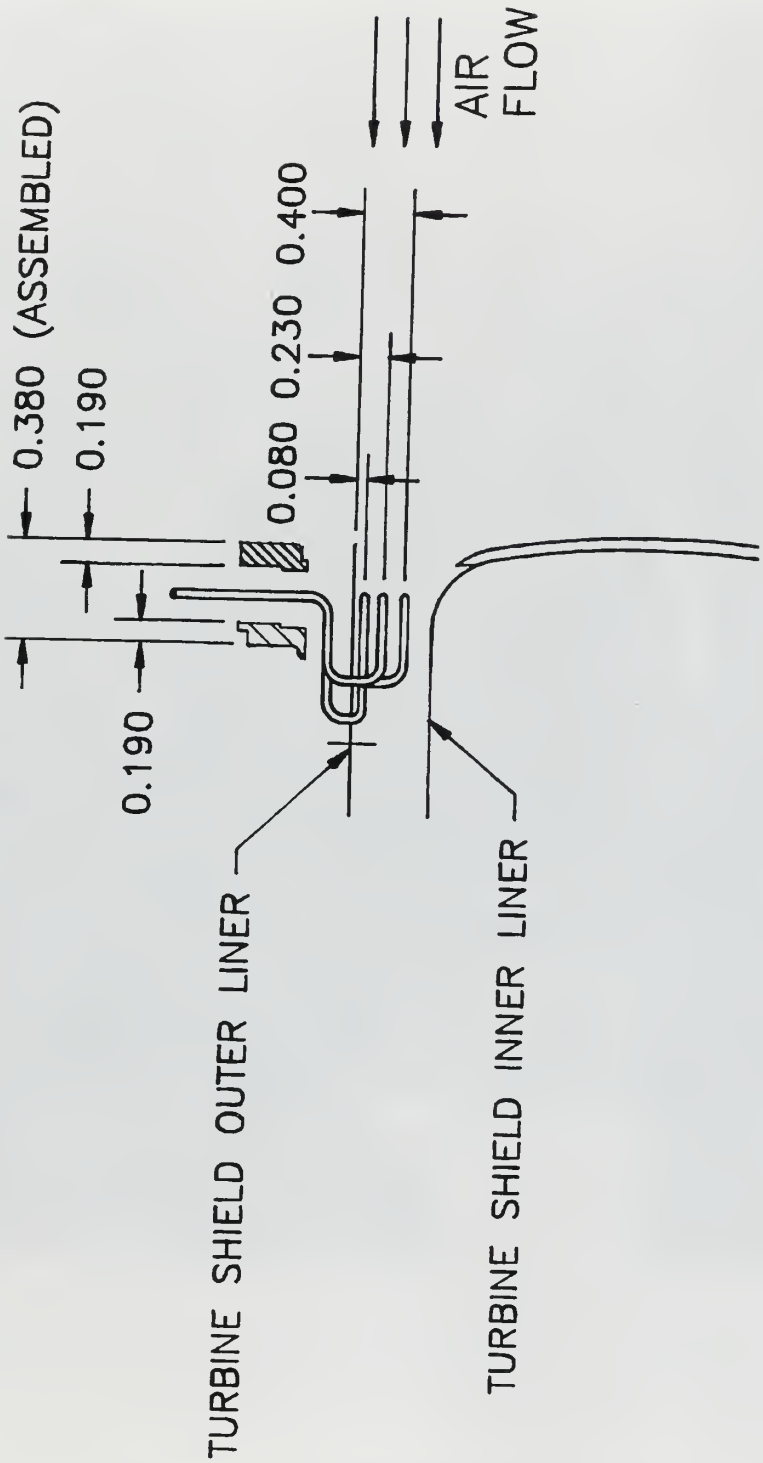

Figure 4.11. Side view of GGT inlet thermocouple ring assembly with thermocouple locations.

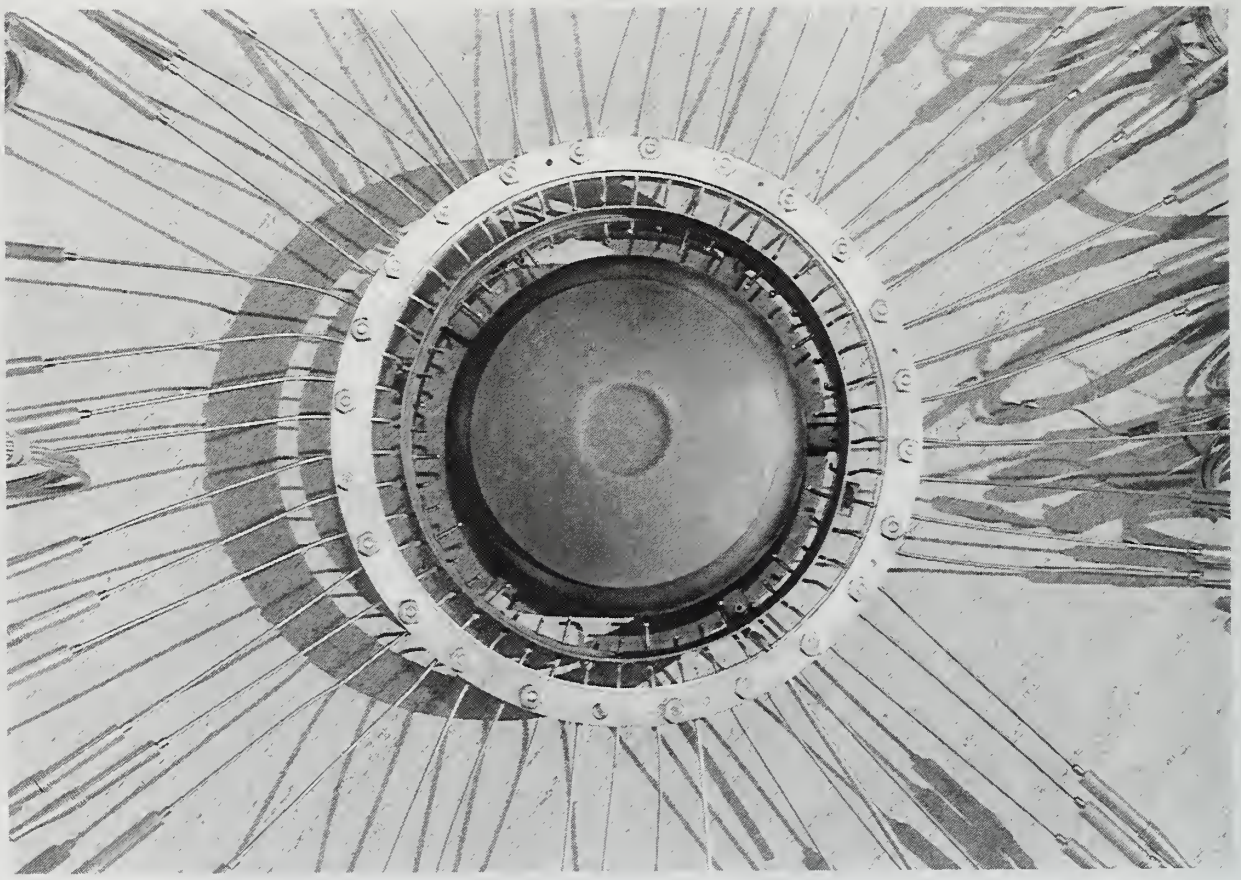

Figure 4.12. Fabricated GGT ring assembly.

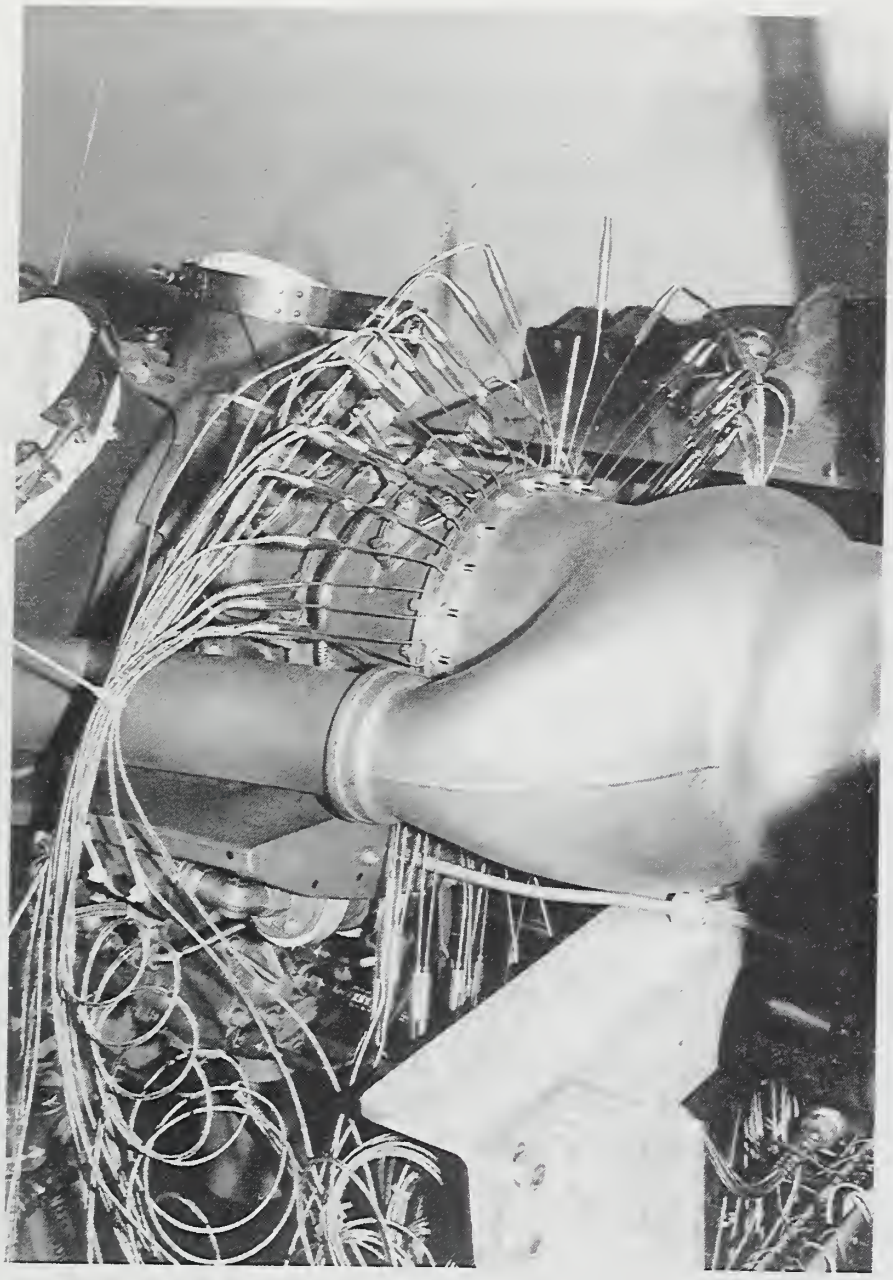

Figure 4.13 Installed GGT ring assembly.

V. ENGINE AND AUXILIARY CONTROL SYSTEMS

The mechanical means of control for the gas turbine engine is accomplished by the SF-901 Engine Dynamometer System manufactured by Superflow Corporation, Colorado Springs, Colorado. This mechanical system in turn is commanded by a control console located outside the engine test cell. The primary engine controls monitored and/or adjusted from the Superflow console are:

1. Engine throttle control
2. Dynamometer load control
3. Support systems monitoring and control.

The safe operation of the engine is accomplished by operating procedures discussed at the end of this chapter and contained in Appendix B.

A. ENGINE THROTTLE CONTROL

The THROTTLE CONTROL knob located on the control console (Figure 5.1) schedules the amount of fuel delivered to the engine via a lever arm assembly located on the gas generator fuel control governor. The lever arm on the gas generator is moved via a throttle actuator located on the engine test stand as shown in Figure 5.2. The gas generator turbine fuel control governor in turn utilizes a bypass valve, a metering valve, an acceleration bellows, a governing and enrichment bellows, a manually operated cutoff valve, and a maximum pressure relief valve to schedule fuel to the combustion chamber.

Fuel is discharged from the engine fuel pump and internal filtering assembly into the fuel control and is directed to the metering valve. The bypass valve maintains a constant differential pressure across the metering valve and bypasses excess fuel back to the engine fuel pump and filter assembly. The metering valve is controlled by lever action through movement of the governor and acceleration bellows. The extent to which the metering valve opens determines the fuel flow to the combustion chamber.

The power turbine also has a fuel governor which is scheduled by the power turbine governor (N2). The governor regulates spring loaded flyweights similar to the action described in the gas generator turbine. These flyweights in turn control the fuel metering valve in the gas generator governor as the power turbine reaches the flight speed. This is accomplished by the use of bleed air from the compressor discharge. The discharge pressure of the compressor is sensed by the power turbine fuel governor. As the desired speed of the engine is approached, the flyweights move to open a link to the power turbine governor orifice. The opening of this orifice sends a small amount of bleed air from the compressor to the gas generator governor. The increase in pressure to the gas generator governor is inversely proportional to gas generator turbine speed by regulating the metering valve within the gas generator governor fuel control. This increase in pressure from the power turbine governor thus decreases the fuel flow to the combustor, slowing the gas generator turbine's speed. [Ref. 1: p. 1.13-1.14]

The sensitivity of the power turbine governor control (N2) is maintained by a lever arm assembly located on the power turbine governor. The position of the arm may vary between a MIN and MAX position on the arm. The MIN position gives the power turbine

governor the greatest sensitivity to gas generator turbine speed. With the power turbine lever arm set to the MIN position the power turbine speed is controlled to a maximum of 35,000 RPM, which in turn produces an output shaft speed of 6,000 RPM. The MAX position, however, is the least sensitive to power turbine speed. This position will allow the power turbine to reach its maximum continuously rated RPM of 36,729 at which point it rapidly closes the fuel metering valve in the gas generator fuel control. This rapid closing of the fuel metering valve prevents the overspeed of the power turbine.

For the ME 3241 course the power turbine governor has been locked into the MAX position in order to allow full control of the power turbine by the water brake dynamometer. The gas generator fuel control (N1) has been directly coupled to the THROTTLE CONTROL knob located on the control console.

B. DYNAMOMETER LOAD CONTROL

In order to utilize the T63-A-700 gas turbine engine in the ME3241 course and conduct engine performance evaluation, the gas generator speed is required to remain fixed while varying the output shaft speed and in turn the power turbine speed. The T63-A-700 gas turbine engine is designed for use in helicopters, in which the speed of the aircraft is not controlled by an increase in rotor speed and thus an increase in power turbine speed. Rather, the speed of the aircraft is controlled by the angle of attack on the rotor blades, thus increasing the load, but not the speed of the power turbine. To overcome the engine's desire to maintain a constant output shaft speed, the water brake

dynamometer varies the speed of the output shaft by changing the torque applied to the shaft.

The speed of the output shaft is controlled at the control console by the LOAD CONTROL knob. The load control operates in two modes, MANUAL and SERVO. In MANUAL mode, the load control maintains a constant torque on the engine regardless of speed. When operated in SERVO mode, the load is variable and a constant output shaft speed is maintained regardless of throttle position.

The load to the output shaft is varied by the Superflow power absorption unit. On the power absorption unit "...a variable water valve, which is located at the absorption unit discharge, regulates the discharge of water from the power absorber to maintain the required pressure within the absorber for proper load control." [Ref. 7: p. 27] A capacity valve on the power absorption unit is used to adjust the sensitivity of the absorption unit. The power absorption unit and the capacity valve are shown in Figure 5.3.

C. SUPPORT SYSTEMS MONITORING AND CONTROL

Three primary support systems are required for the operation of the T63-A-700 gas turbine engine. First, a fuel service system is required to deliver fuel to the engine's internal fuel pump. Second, a complete starter/generator circuit is required for initial rotation of the compressor and charging of two 12 VDC batteries. Finally, engine oil cooling for the gas turbine engine's synthetic oil is required to ensure proper lubrication and cooling of engine internals.

1. Fuel Oil Service System

"The fuel oil service system consist of a fuel filter, pump, accumulator, and flow sensors for two parallel fuel outlets. The two parallel outlets are available for dual injection and dual carburetor systems. Since the gas turbine fuel control has only one fuel line available, the second fuel line is not utilized. The fuel service system receives fuel from the fuel transfer system through two Fram filters. The fuel then enters the inlet of the fuel pump trough a 10 micron filter mounted on the engine test stand." [Ref. 7: p. 35]

From the fuel pump and the 10 micron filter, the fuel then flows into the accumulator through a turbine flow meter and directly into the gas turbine engine. The original design did not allow the operator to rapidly shut off fuel to the engine in the event of an emergency. To allow for the rapid securing of fuel to the engine, the fuel service system design is modified to incorporate a fuel oil solenoid valve located on the discharge side of the turbine flow meters just prior to entering the engine.

The quick acting fuel solenoid valve is a MS-142DC made by the Whitey Company of Cleveland, Ohio. Figure 5.4 displays the circuit schematic designed for the fuel solenoid valve. Operation of the valve is made possible by the use of two separate voltage signals. A 12 VDC signal is used as a control signal to electric relays located in the solenoid valve. When switched these relays provide 24 VDC to a small direct current motor that opens and closes the valve. Power is constantly provided by the two 12 VDC batteries located on the engine test stand. The 12 VDC control signal is connected in parallel with the dynamometer fuel pump power signal. The dynamometer fuel pump switch is located on the control console. In the event of the loss of electrical power to the

control console the solenoid valve's internal relays will de-energize, shutting off fuel to the engine. In the event of an engine casualty the fuel is rapidly secured by simply turning off the dynamometer fuel pump from the control console.

2. Starter/Generator Circuitry

Figure 5.5 contains the electrical schematic diagram designed for use with the T63-A-700 gas turbine engine starter/generator circuitry. The purpose of the system design is to provide electrical power to the starter/generator for initial excitation of the compressor until the engine combustion is self-sustaining. Upon completion of engine start the starter / generator charges the storage batteries via a voltage regulator.

a. Starter Circuitry

The engine starter is energized by depressing the STARTER push-button on the dynamometer control console. Depressing the STARTER push-button provides 12 VDC to relays R1 and R3. The closing of relay R1 completes the circuit for 24 VDC to the starter. With 24 VDC now being supplied to the starter, current flows into the field windings and engine rotation begins . The closing of relay R3 enables 24 VDC power to the exciter ignitor. As the gas generator turbine reaches idle speed (30,000 - 32,000 RPM), the STARTER push-button is released and relays R1 and R3 return to their normal open position. The release of the STARTER push-button ends the start sequence for the gas turbine engine and initiates the generator circuitry.

b. Generator Circuitry

The heart of the generator circuitry is the Generator Control Unit (GCU). All regulation of voltage and thus current to the batteries is accomplished by this unit. With the release of the STARTER push-button the generator circuitry begins to charge the two 12 VDC batteries located on the engine test stand. The completion of the start sequence is detected by terminal "C" on the GCU by monitoring the 12 VDC control signal provided to the exciter ignitor relay and through terminal "D" by sensing the amount of current in the field windings. Upon the loss of the 12 VDC signal to terminal "C" and with the required electrical current in the field windings of the motor sensed at terminal "J," the GCU then regulates the current to the storage batteries. The amount of current to the batteries is sensed through terminals "D," "M," and "G" on the GCU. Terminal "D" senses current flow to the batteries, while terminals "M" and "G" regulate the amount of current to the storage batteries. Switch SW1 is located on the engine test stand next to the storage batteries and is manually operated in the open or close position to allow the operator the ability to disable the charging circuitry if necessary.

3. Lube Oil Storage and Conditioning System

The T63-A-700 gas turbine engine utilizes a circulating dry sump system with supply and scavenge elements enclosed within the engine's accessory gear box. The support function of the lubrication storage and conditioning assembly is to provide a means of storing, cooling, and initial filtering of the MIL-L-23699 lubricating oil.

In designing the lubrication oil storage and conditioning system three main design requirements were originally considered. First, the system must have at a minimum the storage capacity of six quarts of lubricating oil. Second, the system must be able to maintain an oil inlet temperature to the engine of less than 225 °F. Finally, the dynamometer test system must be successfully instrumented for proper monitoring of system pressure and temperature.

The initial system design provided for the proper amount of storage space for the lubricating oil and the measurement of the lubricating oil's temperature and pressure were properly monitored. [Ref. 7] However, two problems were identified in testing. First, the original design did not provide any filtering of the oil prior to entering the engine. Second, the original oil cooler used for cooling was found to be inadequate. Therefore a design modification was necessary.

a. Filter Assembly

Filtering of the oil prior to engine entrance is accomplished by placing a Fram oil filter (PH-13) on the discharge side of the lubrication oil storage tank just prior to the engine inlet. The filter removes all large particulate matter up to 45 microns. The oil inlet temperature to the engine is measured by placing a thermocouple connection within the oil filter assembly.

b. Oil Cooler Modification

The original oil cooler used for the cooling of the lubricating oil was a radiator, fin type heat exchanger which utilizes forced air from a gear driven fan to cool

the lubricating oil. In the helicopter airframe, the gear-driven fan was powered by shafting from the tail rotor transmission assembly. In the gas turbine engine test cell the tail rotor shafting connection of the engine is used to drive the main drive shaft to the dynamometer power absorber and thus cannot be used as a power source for the lubricating oil cooler fan. To overcome this problem an electric fan was mounted behind the oil cooler providing 200 CFM of air for cooling of the oil.

Although the original design provided adequate cooling of the lubricating oil with the engine in the flight idle position (N1 = 30,000 - 32,000 RPM), the heat capacity of the oil cooler was quickly overwhelmed at high power settings and allowed the oil inlet temperature to the engine to exceed 225 °F. To increase the heat transfer rate between the air and the oil two possible design modifications were considered. First, a design to increase the amount of air flowing through the oil cooler was considered. Second, the use of a larger oil cooler and thus an increased heat capacity was studied. Because of space limitations on the engine test stand and the availability of a UH-1 helicopter oil cooler, the second design modification was selected.

(1) UH-1 Oil Cooler Analysis

The UH-1 oil cooler assembly is a radiator, fin type, single-pass, cross-flow heat exchanger. The assembly consists of two separate heat exchangers; used in the UH-1 helicopter for engine oil cooling and rotor transmission oil cooling. The UH-1 oil cooler assembly is modified for the T63-A-700 gas turbine by putting the two oil

coolers in series with each other with airflow provided by the electric blower. Figure 5.6 shows the modified cooler assembly mounted on the engine test stand.

The objective of the oil cooler assembly is to maintain the temperature of oil entering the engine below 225 °F at all power settings. The maximum amount of heat rejected to the oil occurs at full power on the engine. For this reason the analysis of the oil cooler assembly is done at full power. The following is a list of inlet conditions and assumptions.

1. Air inlet temperature - $T_{air,in} = 70$ °F.
2. Engine heat rejection rate into the oil - $Q_{engine} = 566$ BTU/min. [Ref. 1]
3. Maximum oil outlet temperature of the oil cooler assembly - $T_{max} = 225$ °F. [Ref. 1]
4. With the transmission cooler covering only one quarter of the total frontal area of the oil cooler assembly and the lube oil cooler using the remaining three quarters, the total air flow rate is proportioned based on frontal areas as follows: $\dot{m}_{air,tran} = 50CFM$; $\dot{m}_{air,lube} = 150CFM$.
5. Engine oil flow rate at full power - $\dot{m}_{oil} = 3.06GPM$ [Ref. 1]

Figure 5.7 and Figure 5.8 contain the heat transfer curves for the transmission oil and lubricating oil coolers, respectively. Using 225 °F as the maximum allowable

temperature of the oil to the engine an outlet temperature of the oil may be calculated using the energy balance equation as shown below:

$$T_{oil,out} = T_{oil,in} + \frac{Q_{engine}}{\dot{m}_{oil}\, c_{p,oil@225F}} \tag{5.1}$$

The oil outlet temperature along with other parameters of the oil are contained in Table 5.1. Table 5.2 displays the parameters assumed and known for the air flow through the two heat exchangers. With the data found in Table 5.1 and Table 5.2, heat transfer rates are obtained from the graphs for each heat exchanger. For both charts the left-hand ordinate gives the heat rejection in term of BTUs per minute per 100 °F Inlet Temperature Difference (ITD). To obtain the actual heat transfer rate for a given ITD, air flowrate, and oil flowrate, multiply the heat rejection rate read from the curve by the ITD and then divide by 100 °F as shown below:

$$Q_{act} = Q_{read} \frac{(T_{hot,in} - T_{cold,in})}{100} \tag{5.2}$$

In this equation $T_{hot,in}$ and $T_{cold,in}$ represent the temperatures of the oil entering the heat exchanger and the air entering the heat exchanger, respectively. To determine the actual heat transfer rate for both heat exchangers the oil inlet temperatures ($T_{hot,in}$) must be determined. The modified oil cooler assembly has been fabricated such that the lubricating oil from the engine will first encounter the transmission oil cooler. An outlet temperature of the lubricating oil from the transmission oil cooler is obtained by again an energy balance as shown below:

$$T_{tran,out} = T_{oil,out} - [\frac{\dot{Q}_{act,tran}}{\dot{m}_{oil}\, c_{p,oil@272.1F}}] \quad (5.3)$$

With both oil inlet temperatures known, Figures 5.7 and 5.8 are entered and the actual heat transfer rates calculated. These calculations are shown in Table 5.3.

The total heat transfer rate for the modified lube oil cooler is 720.07 BTU/min. This number exceeds the heat rejected by the engine into the oil (566 BTU/min). Therefore, it can be concluded that the temperature of the oil entering the engine will never exceed the maximum of 225 °F and the design modification is satisfactory.

However, during actual testing of the system the oil temperature exceeded the maximum oil temperature of 225 °F within 15 minutes of the engine running at full power. Because a larger oil cooler was installed upstream of the blower fan the required amount of air flow for the cooler could not be met by the fan. With these test results in mind, a new fan blower has been ordered to ensure at least 200 CFM of air through the oil cooler assembly. As of this writing the new fan has not been delivered or installed.

D. ENGINEERING OPERATING PROCEDURES

To ensure the safe and proper operation of the T63-A-700 gas turbine engine and its support equipment Standard Operating Procedures (SOP) were developed in Ref. 7. The physical verification of these procedures and validation of decision making processes for engine control were not conducted before printing of these operating guidelines.

Appendix B contain the validated and verified Standard Operating Procedures of Ref. 7. The SOP is subdivided in five procedures as listed below:

1. Master Light Off Procedure (MLOP)
2. Fuel Oil System Recirculation Procedure (FOSRP)
3. Cooling Water System Recirculation Procedure (CWSRP)
4. Normal Shutdown Procedure (MNSP)
5. Emergency Shutdown Procedure (ESP)

Mass Flowrate $(\dot{m}_{oil})$ *[lbm/min]*	*Specific Heat (cp) [BTU/lbm-°F]*	*Specific Gravity* (γ)	*Engine Oil Inlet Temp* $(T_{oil,in})$ *[°F]*	*Engine Oil Outlet Temp* $(T_{oil,out})$ *[°F]*
23.28	0.516	0.914	225	272.1

Table 5.1. Engine oil particulars.

Air Inlet Temp. $(T_{air,in})$ *[°F]*	*Total Air Mass Flowrate* $(\dot{m}_{air,tot})$ *[lbm/min]*	*Transmission Cooler Air Mass Flowrate* $(\dot{m}_{air,tran})$ *[lbm/min]*	*Lubricating Cooler Air Mass Flowrate* $(\dot{m}_{air,lub})$ *[lbm/min]*
70.0	15	3.75	11.25

Table 5.2. Cooling air particulars.

Transmission Cooler Oil Inlet Temp $(T_{tran,in})$ *[°F]*	*Lubricating Oil Cooler Inlet Temp* $(T_{lube,\ in})$ *[°F]*	*Heat Transfer Rate (Trans. Cooler)* (Q_{tran}) *[BTU/min]*	*Heat Transfer Rate (Lub. Cooler)* (Q_{lube}) *[BTU/min]*	*Total Heat Transfer Rate* (Q_{total}) *[BTU/min]*
272.1	259.5	151.57	568.5	720.07

Table 5.3. Calculated temperatures and heat transfer rates for modified UH-1 lube oil cooler.

Figure 5.1. T63-A-700 control console.

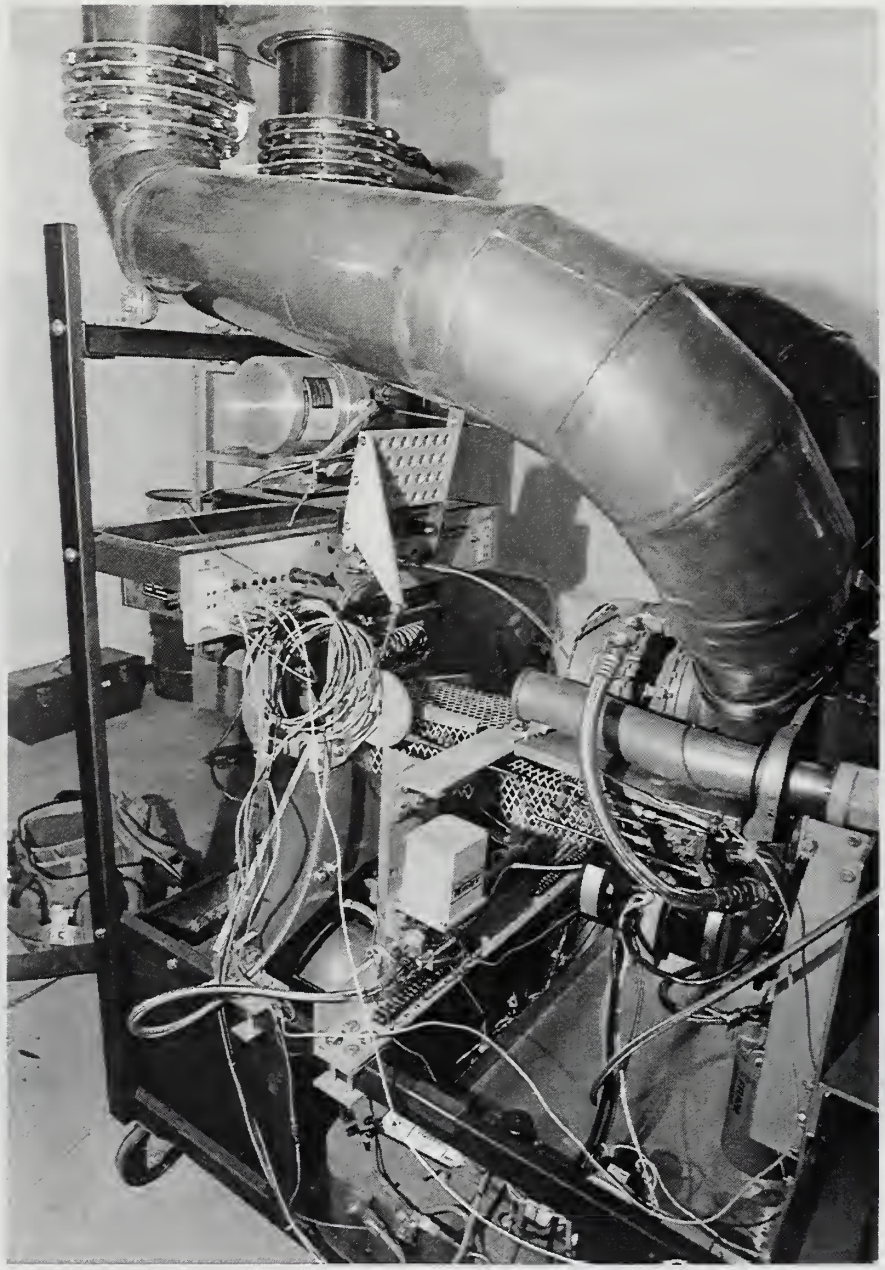

Figure 5.2. N1 (GGT) throttle arm linkage assembly.

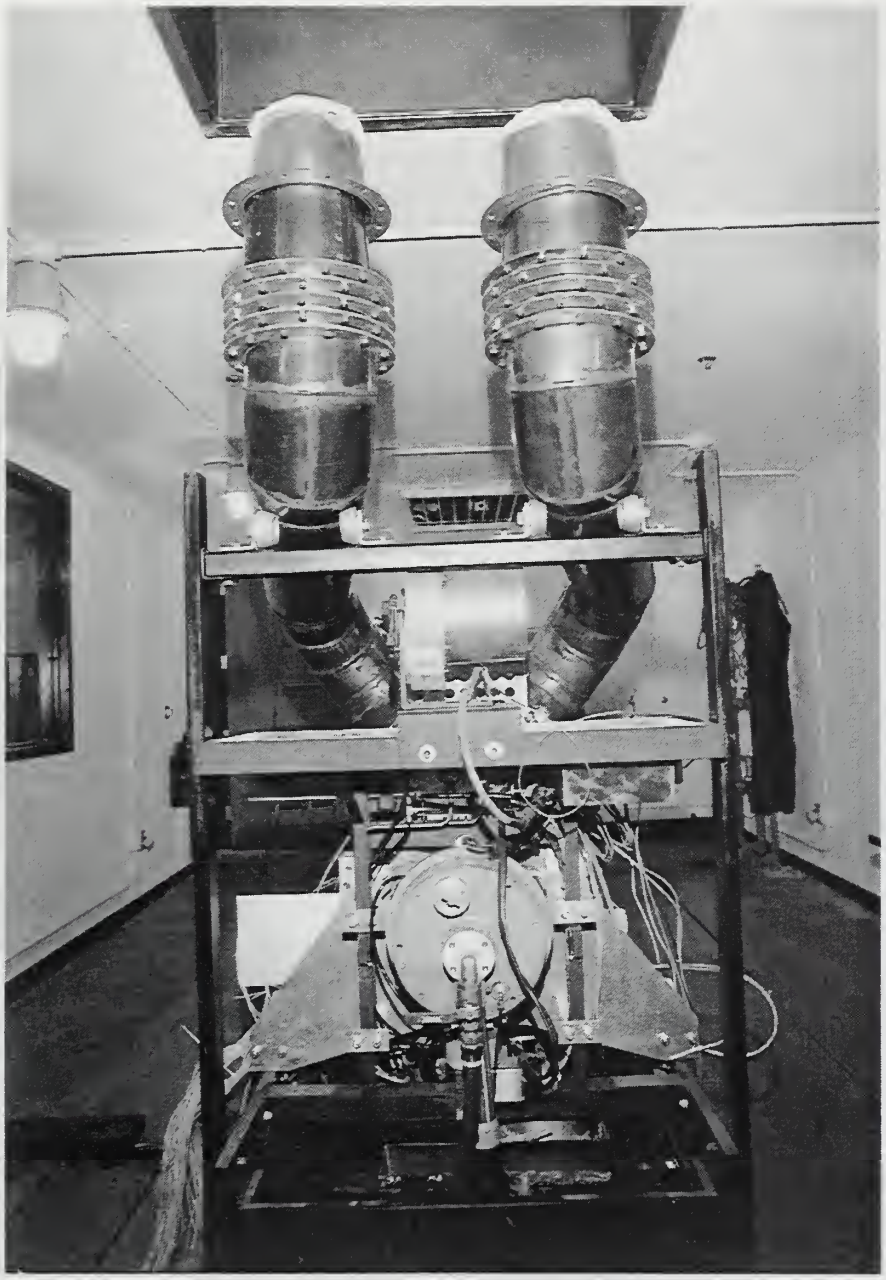

Figure 5.3. Power absorption unit with capacity valve.

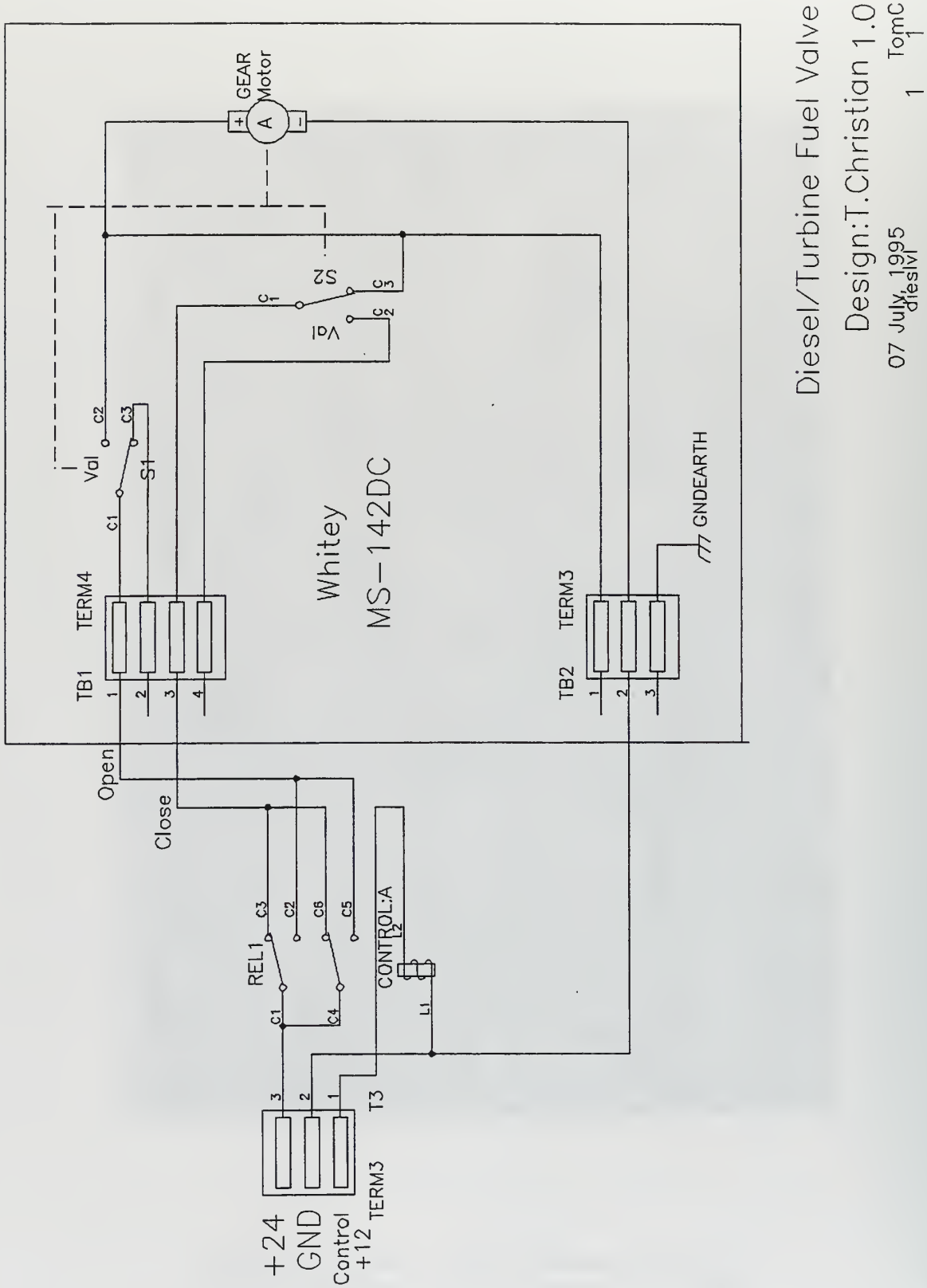

Figure 5.4. Whitey fuel oil solenoid valve electrical schematic diagram "From Ref. [8]."

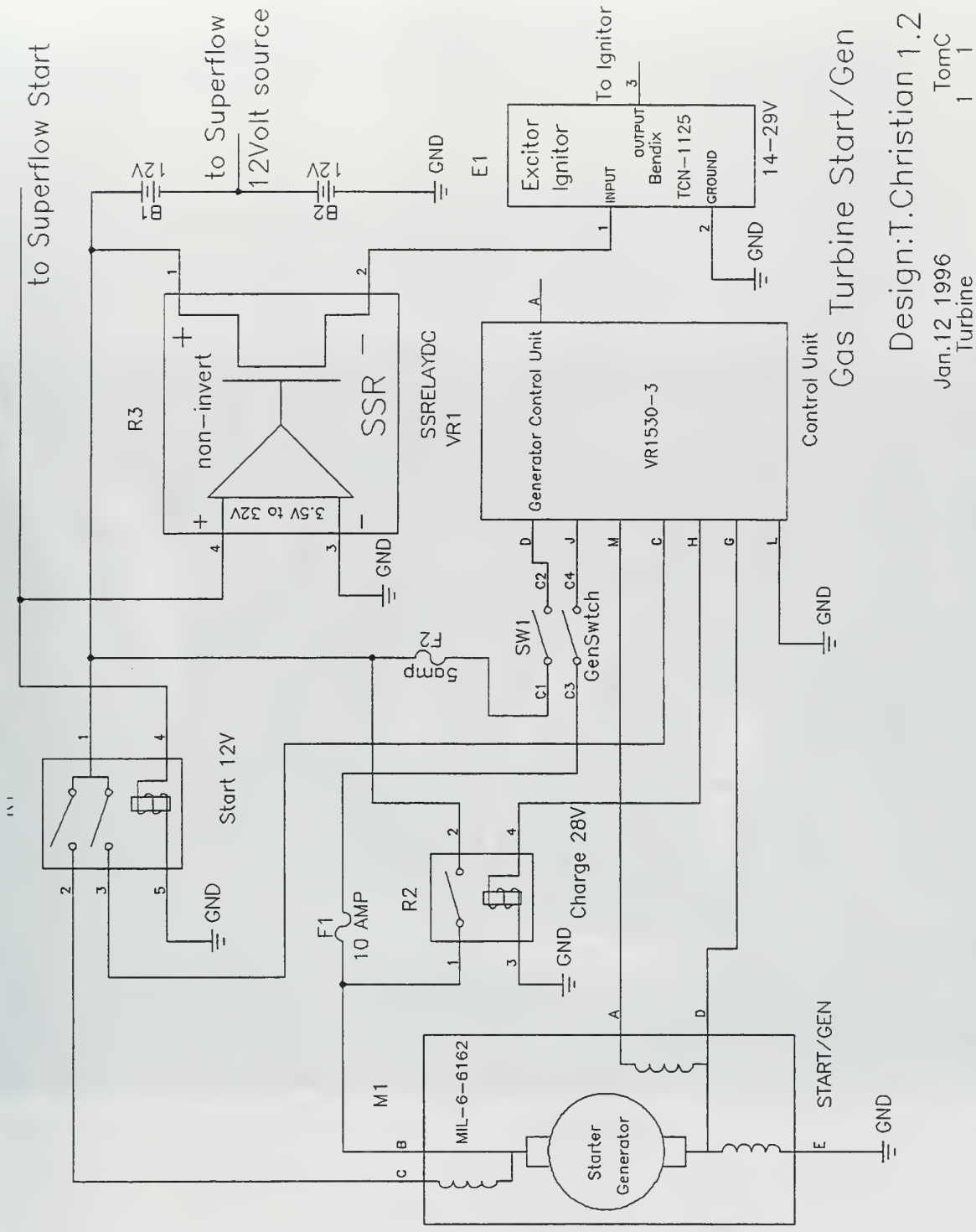

Figure 5.5. Starter/Generator electrical schematic diagram "From Ref. [8]."

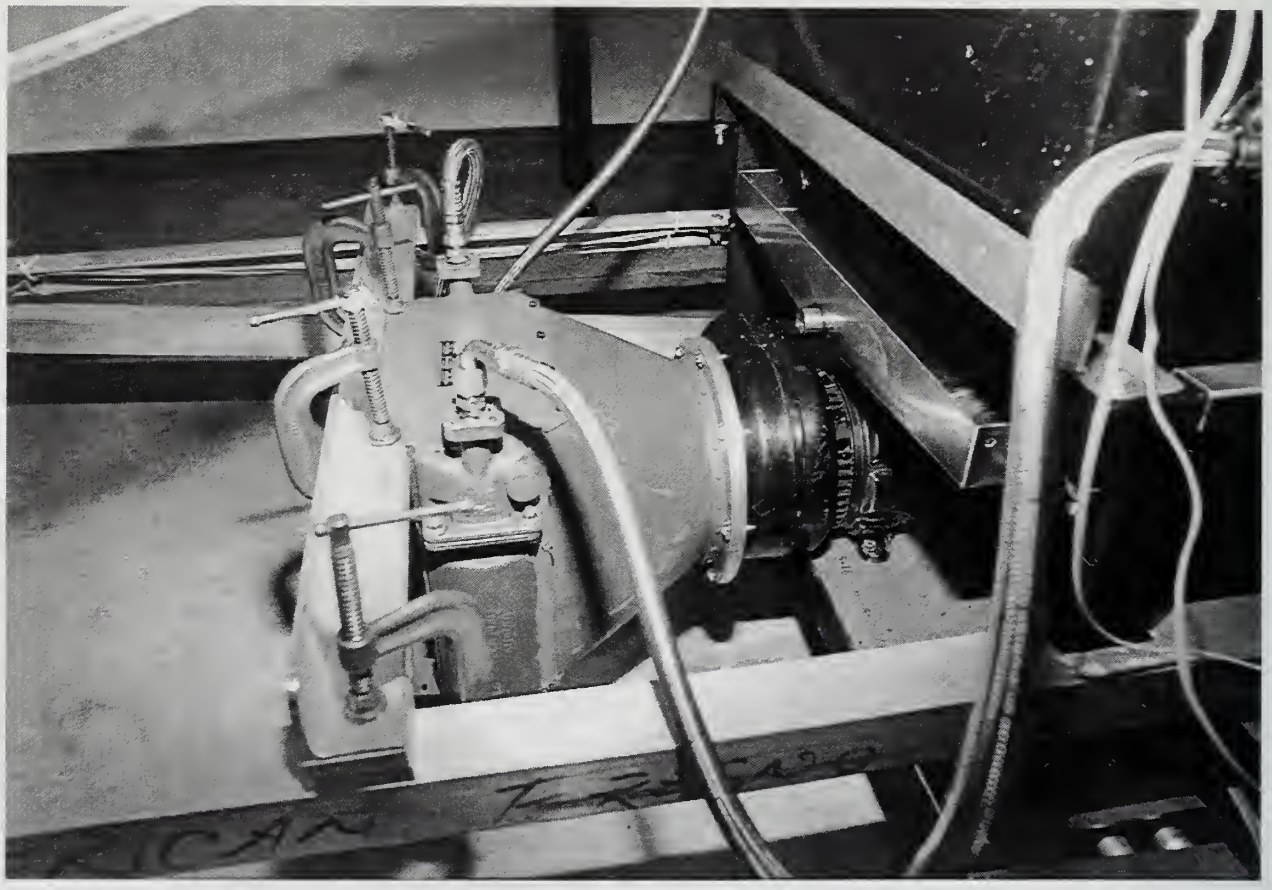

Figure 5.6. Modified UH-1 oil cooler assembly.

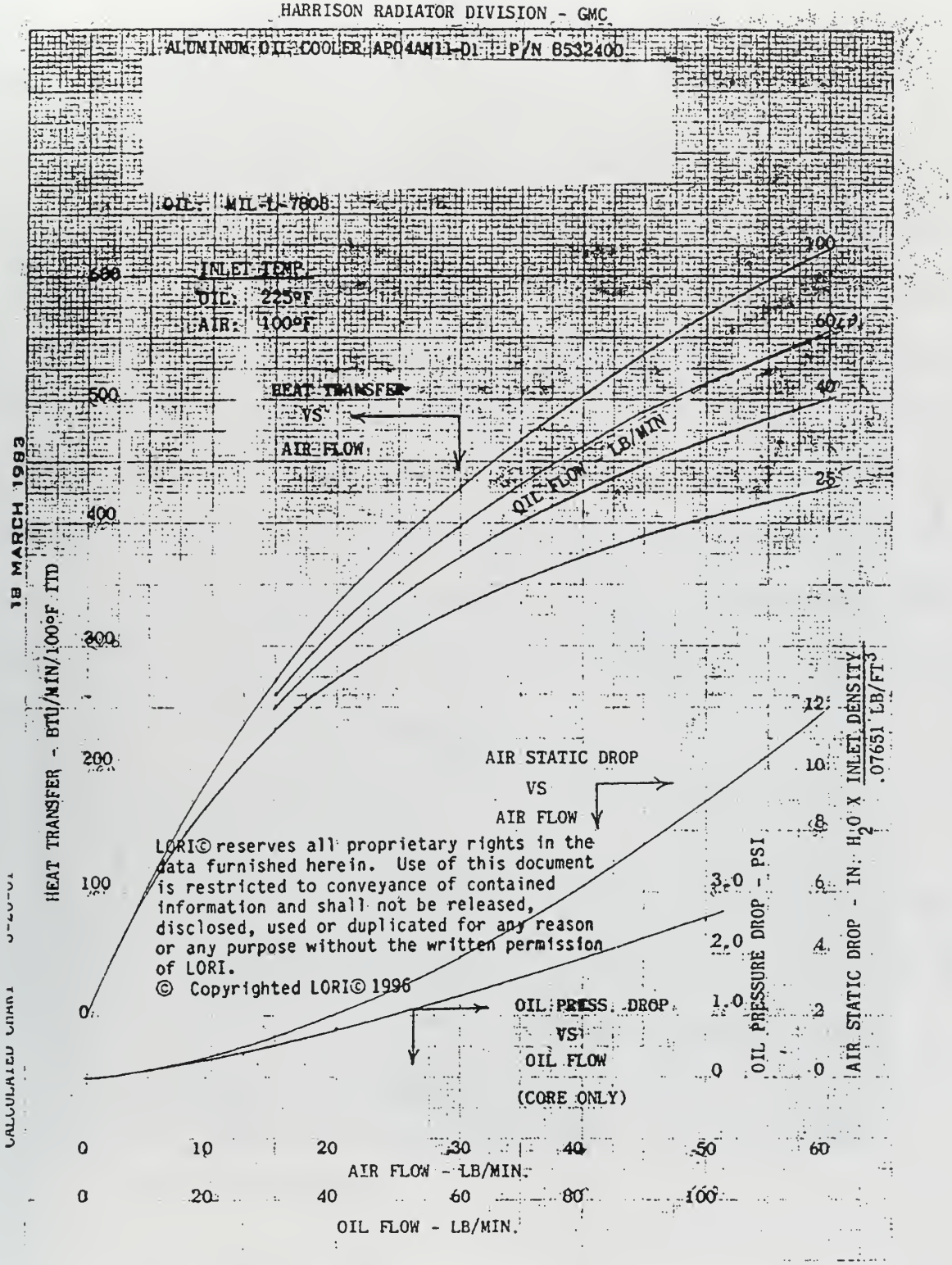

Figure 5.7. UH-1 transmission oil cooler heat transfer curves. "From Ref. [9]."

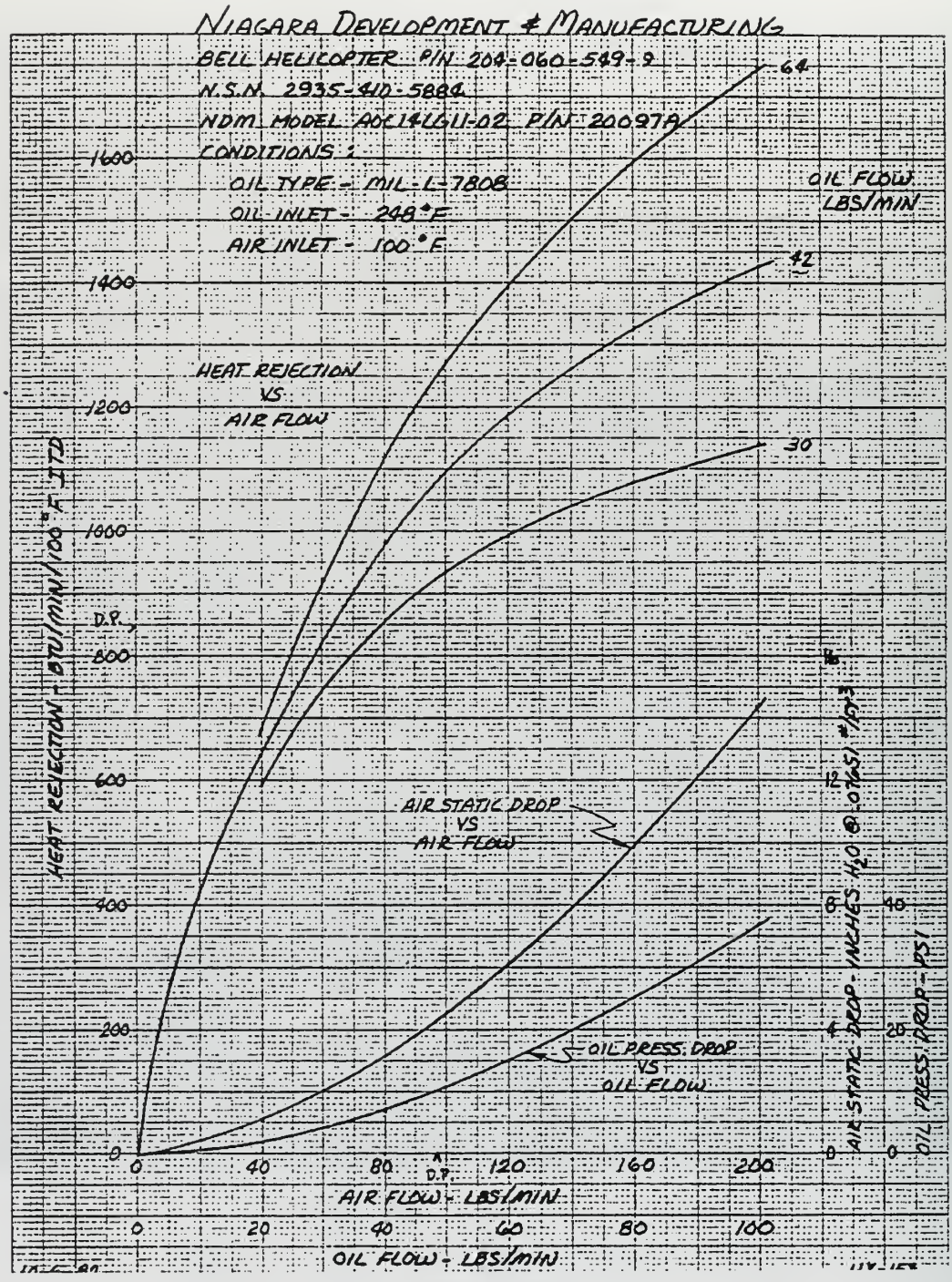

Figure 5.8. UH-1 lubricating oil cooler heat transfer curves. "From Ref. [10]."

VI. TESTING AND EVALUATION

A. TESTING PROCEDURE

To evaluate the performance of the instrumentation package installed on the engine a test was developed to examine the accuracy of the newly installed instrumentation and compare the results of this data against the engine model supplied by Allison Engine Corporation, Superflow test results, and the Allison installation manual. The testing procedure required the gas generator turbine speed remain fixed while varying the output shaft speed. The testing was conducted at the maximum continuous speed of the gas generator turbine of 49,760 RPM as per the installation manual. [Ref. 1] The output shaft speed was increased in 250 RPM increments from 4,000 RPM to 6,000 RPM. At each different output shaft speed a complete set of temperature, pressure, flow rate, and engine speed readings were collected.

B. ACQUISITION SYSTEMS

The collection of data is accomplished by two separate monitoring systems. First, the Superflow 901 system collects data and has some limited capabilities to process the data received. The useful parameters computed by the Superflow system are:

1. Brake Specific Fuel Consumption
2. Output shaft horsepower
3. Output shaft speed in RPM
4. Fuel mass flow rate

5. Air volumetric flow rate

6. Fuel to air ratio

The second monitoring system utilizes both a Hewlett Packard HP3852A Data Acquisition Control Unit and a Unitek 486 personal computer. The HP3852A Data Acquisition Control Unit collects 56 temperature and 9 pressure readings at various state points throughout the engine. These recorded values are then stored and processed by the Unitek 486 personal computer. To simplify the instrumentation monitoring, both the Superflow monitoring system and the Hewlett Packard - Unitek system are electronically coupled in order to simultaneously collect and store data. The coupling is accomplished by use of a trigger signal sent from the Superflow control console to the HP3852A Data Acquisition Unit. Additionally, a test sequence is programmed within the Superflow console to allow the operator the ability to press a single push button and run the entire engine test.

The post processing of the data is accomplished by the MATLAB program found in Appendix C. The following is a list of results obtained from the data collected by the Hewlett Packard - Unitek system:

1. Compressor, Gas Generator Turbine, and Power Turbine Work

2. Compressor, Gas Generator Turbine, and Power Turbine adiabatic efficiencies

3. Brake Specific Fuel Consumption

4. Thermal Efficiency

5. Gearbox Efficiency

C. TEST SUMMARY AND COMPARISONS

Table 6.1 contains the predicted engine performance from the engine model provided by Allison Engine Corporation. Table 6.2 contains the state point average temperatures calculated by the MATLAB program from Appendix C. Table 6.3 and Table 6.4 contain the engine behavior and performance characteristics based upon the measured temperature and pressure readings collected by the Unitek system. Table 6.5 displays the engine performance characteristics found from the Superflow system.

Several comparisons of the data presented in the tables can be made. This section looks at the following comparisons:

1. State point comparison
2. Brake specific fuel consumption and thermal efficiency
3. Component work
4. Component adiabatic efficiencies
5. Gas generator inlet temperature

1. State Point Comparison

Table 6.1 contains the engine model data provide by Allison Engine Corporation. The Allison data provides temperature and pressure readings for the gas turbine by varying the gas generator turbine speed (N1) and maintaining the power turbine speed (N2)

constant. Table 6.2 presents the measurement data taken during the actual engine test. The state point comparison in Table 6.3 compares the recorded measurements taken during testing at the peak output shaft speed (6,000 RPM) to the Allison data at a similar speed. Additionally, percent differences between measured and predicted values are presented.

Nearly all measured parameters are roughly equal with the predicted engine data of Table 6.1. Table 6.3 reveals, however, two questionable values in the measurement of the state points. Specifically, the measurements of compressor discharge pressure (P_{T2}) and gas generator inlet pressure (P_{T4}) are not within acceptable limits from the predicted values.

The lower discharge pressure measurement taken during testing is due to the location of the Kiel - probes within the compressor. Because the access to the compressor discharge is limited, both Kiel - probes are placed at bleed air ports not in use on the centrifugal compressor casing. The locations of these ports are equidistant from the true discharge of the compressor, ensuring the two pressure measurements are close in magnitude. However, because the probes are not precisely at the discharge of the compressor, but within the centrifugal compressor casing itself, some of the air that is being compressed is not measured by the Kiel probes causing a lower pressure reading for calculations.

The most likely cause to a lower than predicted value of total pressure at the gas generator turbine inlet is due to a malfunction of a pressure transducer at the time of testing. Of the two pressure transducers located on the ring assembly one was found to be

inoperable creating a loss of redundancy for the pressure measurement at that point and decreasing the accuracy.

2. Brake Specific Fuel Consumption and Thermal Efficiency

Table 6.4 presents the comparison of the three separate values for the brake specific fuel consumption at the peak test speed. The specific fuel consumption from the Superflow system is consistently higher because it is based upon the measured mechanical shaft horsepower instead of the power turbine work as in the engine model data and the computed specific fuel consumption from the measured data.

The Superflow system does not directly compute thermal efficiency. However, using the relationship found in Equation 6.1, a derived value from the Superflow data is calculated and listed in Table 6.4.

$$\eta_{th} = \frac{2544.43}{\dot{m}_f \, Q_R} \tag{6.1}$$

For Equation 6.1 the units of the fuel mass flow rate are pounds mass per hour, while the lower heating value has units of BTUs per pound mass. A conversion factor of 2544.43 is necessary to ensure the efficiency is dimensionless.

The predicted thermal efficiency, computed thermal efficiency and the Superflow derived thermal efficiency are all similar. This again shows that for this power setting the instrumentation installed matches the predicted values.

3. Component Work

The comparison between predicted compressor, gas generator turbine, and power turbine work and the computed measured work is presented in Table 6.5. Additionally, for the power turbine, the measurement of the output shaft horsepower as measured by the Superflow system along with a gearbox efficiency is displayed. In general the work of the gas generator turbine is always the largest value for it powers the compressor and the accessories gearbox. The power turbine work listed for the predicted model in Table 6.5, is larger than the measured work because the engine model power turbine speed is slightly larger than the speed used for the test. In the model the power turbine speed is at 105% rated speed (36,729 RPM). This increase in speed increases the amount of horsepower delivered by the power turbine and for this reason is roughly 7% higher than the measured power turbine work.

The power turbine work for the predicted engine model and computed work from measurements is greater than that of the work found by the Superflow system. This is due to the losses encountered in the reduction gear from power turbine to the output drive shaft. The gearbox efficiency is the ratio of these two power readings.

4. Component Adiabatic Efficiencies

The comparison of adiabatic efficiencies is drawn from the data in Table 6.1 and Table 6.. The model data presented in Table 6.1 unfortunately is of limited use for the comparison of the Power Turbine efficiency due to the fact that the model holds the power turbine speed constant and varies the gas generator turbine speed. For the model data

shown in Table 6.1, the power turbine speed is held at a slightly higher speed than that of the peak test speed of 35,000 RPM (6,000 RPM output drive shaft). Because of this only the efficiencies of the Power Turbine at the peak drive shaft speed of 6,000 RPM can be compared to the engine model. At these speeds the power turbine efficiencies are strikingly similar. The measured power turbine efficiency from Table 6.6 is 85.6% where as for the engine model the corresponding efficiency is 85.0%. Additionally, these two values are within the design goal of 4.5% uncertainty. Therefore, at this power setting the computed efficiency of the power turbine is accurate.

The compressor and gas generator turbine adiabatic efficiencies for the test cycle remain relatively constant. This is due to the fact that both the compressor and the gas generator turbine speeds remain fixed throughout the test cycle. The comparison of the measured efficiencies from Table 6.6 and Table 6.1 for the compressor are alike. The engine model presents a predicted adiabatic efficiency of roughly 74%. From Table 6.3 the computed efficiency from thermodynamic calculations ranges from 72% - 73%. Once again, the computed and predicted efficiency values for the compressor are within the design parameter of 3% uncertainty in efficiency.

The gas generator turbine comparison between predicted and measured efficiency data is not, however, similar. For the measured data of Table 6.3 the gas generator turbine efficiency remains relatively constant between 93% to 95%. Obviously this value is in error. The reason for this error is due in part to a possible measurement error in the total pressure entering the gas generator turbine. The predicted value for the test speed is 83.40 psia from interpolating Table 6.1. From Table 6.2 the measured total pressure

entering the gas generator turbine is 5 psia less than predicted. If the measure efficiency calculation of Table 6.3 used the predicted inlet pressure instead the of erroneous measured value, the gas generator efficiency would decrease from 93% to a value of roughly 90%. This new value approaches the predicted value of 88.3% and would be within the design goal of 3% uncertainty. Additionally, the value of the measured inlet temperature is slightly higher than predicted which in turn decreases the temperature ratio and increases the overall efficiency as shown in Equation 3.3a. Table 6.6 contains the tabulated values for the comparison drawn in this section.

5. Gas Generator Turbine Inlet Temperature

There are two possible means to compare the gas generator turbine inlet temperature. First, a simple comparison of the predicted temperature from Table 6.1 to that of the actual computed value found from the average measured temperature in Table 6.2. The predicted value obtained from Table 6.1 corresponds to a gas generator turbine speed (N1) of 97%. From interpolation and applying a correction for inlet temperatures a value of 2,167 Rankine is calculated. The measured temperature from Table 6.2 corresponding to roughly 6,000 RPM of the drive shaft is 2210.0 Rankine. The difference in these values is 1.98%. This small percent difference, shows that the assumptions made for determining the measured gas generator inlet temperature are reasonable.

The second comparison method uses the energy balance equation shown below:

$$(1+f)h_{T4} = h_{T2} + fQ_R \tag{6.2}$$

In Equation 6.2 h_{T2} and h_{T4} are the total enthalpy per pound mass values at state point 2 and 4, respectively. With enthalpy being proportional to temperature, Equation 6.2 can be simplified to the relationship given below in terms of the gas generator inlet temperature.

$$T_{T4} = \frac{(c_p T_{T2} + f Q_R)}{c_p (1 + f)} \tag{6.3}$$

Using this relationship and assuming a lower heating value of 18,621.26 BTUs per pound mass, a theoretical gas generator inlet temperature of 2158.3 Rankine is computed. This is a 2.40% difference from the computed bulk average value for the gas generator ring assembly. Again, this seems to be reasonably close to the actual measured value and shows again that the calculation used to compute the bulk average gas generator turbine inlet temperature is a fairly good approximation. The values discussed in this section are presented in Table 6.7.

Table 6.8, Table 6.9, and Table 6.10 present additional calculations performed by the MATLAB program found in Appendix C and the Superflow Terminal.

N1 (%)	N2 (%)	ma (lbm/s)	mf (lbm/hr)	rho (lbm/ft^3	Area 2 (in^2)	V @2 (ft/sec)	a@2 (ft/sec)	M@2 (V/a)	
70.000	105.000	1.960	72.000	0.1510	1.563	598.2	1350.799	0.443	
75.000	105.000	2.100	82.000	0.1663	1.563	581.9	1381.024	0.421	
80.000	105.000	2.350	93.000	0.1836	1.563	589.3	1412.036	0.418	
85.000	105.000	2.475	109.000	0.2019	1.563	564.9	1441.532	0.392	
90.000	105.000	2.740	136.000	0.2209	1.563	571.5	1471.697	0.388	
95.000	105.000	2.964	166.000	0.2374	1.563	575.3	1506.230	0.382	
100.000	105.000	3.140	206.000	0.2486	1.563	582.0	1541.337	0.378	
105.000	105.000	3.280	232.000	0.2522	1.563	599.3	1570.978	0.381	

N1 (%)	N2 (%)	Tt1 (R)	Tt2 (R)	Tt4 (R)	Tt5 (R)	Tt6 (R)	Tau (comp)	Tau (ggt)	Tau (pt)
70.000	105.000	520.000	759.400	1401.100	1155.000	1143.9	1.460	0.824	0.990
75.000	105.000	520.000	794.900	1526.600	1249.300	1211.5	1.529	0.818	0.970
80.000	105.000	520.000	831.000	1639.200	1330.800	1255.0	1.598	0.812	0.943
85.000	105.000	520.000	866.700	1743.400	1404.800	1282.6	1.667	0.806	0.913
90.000	105.000	520.000	904.000	1868.900	1499.100	1331.3	1.738	0.802	0.888
95.000	105.000	520.000	947.600	2027.600	1623.500	1409.0	1.822	0.801	0.868
100.000	105.000	520.000	993.000	2202.900	1763.500	1507.5	1.910	0.801	0.855
105.000	105.000	520.000	1032.300	2362.800	1893.400	1606.6	1.985	0.801	0.849

N1 (%)	N2 (%)	Pt1 (psi)	Pt2 (psi)	Pt4 (psi)	Pt5 (psi)	P6 (psi)	Qr(BTU/lbm)		
70.000	105.000	14.696	42.178	40.184	17.329	14.774	18400.000		
75.000	105.000	14.696	48.931	46.685	19.329	14.761	18400.000		
80.000	105.000	14.696	56.470	53.921	21.384	14.821	18400.000		
85.000	105.000	14.696	64.766	61.872	23.542	14.858	18400.000		
90.000	105.000	14.696	73.927	70.697	26.077	14.900	18400.000		
95.000	105.000	14.696	83.268	79.757	28.795	14.944	18400.000		
100.000	105.000	14.696	91.382	87.666	31.171	14.998	18400.000		
105.000	105.000	14.696	96.365	92.576	32.684	15.032	18400.000		

N1 (%)	N2 (%)	pi(comp)	pi(ggt)	pi(pt)	cp (comp)	cp (ggt)	cp (pt)		
70.000	105.000	2.870	0.431	0.853	0.241	0.257	0.253		
75.000	105.000	3.330	0.414	0.764	0.241	0.261	0.256		
80.000	105.000	3.843	0.397	0.693	0.242	0.264	0.258		
85.000	105.000	4.407	0.380	0.631	0.242	0.266	0.260		
90.000	105.000	5.030	0.369	0.571	0.242	0.269	0.261		
95.000	105.000	5.666	0.361	0.519	0.242	0.275	0.265		
100.000	105.000	6.218	0.356	0.481	0.243	0.277	0.269		
105.000	105.000	6.557	0.353	0.460	0.243	0.280	0.271		

N1 (%)	N2 (%)	Comp Eff	GGT Eff	PT Eff	k (comp)	k (ggt)	k (pt)		
70.000	105.000	0.764	0.872	0.230	1.400	1.365	1.365		
75.000	105.000	0.772	0.879	0.435	1.398	1.356	1.365		
80.000	105.000	0.781	0.882	0.614	1.398	1.350	1.362		
85.000	105.000	0.786	0.881	0.760	1.397	1.347	1.359		
90.000	105.000	0.787	0.883	0.821	1.396	1.341	1.355		
95.000	105.000	0.771	0.883	0.845	1.395	1.335	1.350		
100.000	105.000	0.743	0.883	0.850	1.394	1.329	1.344		
105.000	105.000	0.710	0.883	0.850	1.393	1.324	1.338		

N1 (%)	N2 (%)	Wc (BTU/lbm	Wggt	Wpt	SHP	SFC	Thermal Eff	FAR	Ideal Nth
70.000	105.000	57.719	63.248	2.808	7.865	9.154	0.0150	0.0102	0.0817
75.000	105.000	66.333	72.237	9.677	29.057	2.822	0.0485	0.0108	0.1338
80.000	105.000	75.138	81.418	19.556	65.723	1.415	0.0967	0.0110	0.1819
85.000	105.000	83.832	90.068	31.772	112.594	0.968	0.1411	0.0122	0.2247
90.000	105.000	92.966	99.476	43.796	172.086	0.790	0.1726	0.0138	0.2637
95.000	105.000	103.479	111.128	56.843	242.031	0.686	0.1986	0.0156	0.2969
100.000	105.000	114.939	121.714	68.864	311.444	0.661	0.2054	0.0182	0.3215
105.000	105.000	124.489	131.432	77.723	367.695	0.631	0.2150	0.0196	0.3348

Table 6.1. T63-A-700 predicted thermodynamic performance. "From Ref. [11] with permission from Allison Engine Co."

Designed Shaft Speed [RPM]	T_{t1} [R]	T_{t2} [R]	T_{t4} [R]	T_{t5} [R]	T_{t6} [R]	P_{t1} [psia]	P_{t2} [psia]	P_{t4} [psia]	P_{t5} [psia]	P_6 [psia]
4,000	537.95	986.46	2230.8	1779.8	1566.0	14.848	80.331	77.432	29.60	15.11
4,250	537.49	983.91	2210.0	1759.3	1525.7	14.847	80.070	77.487	29.43	15.14
4,500	537.47	983.50	2205.8	1761.4	1507.5	14.850	79.611	77.636	29.27	15.10
4,750	538.72	983.02	2197.1	1751.6	1504.8	14.854	79.202	77.214	29.20	15.07
5,000	540.04	984.79	2210.1	1764.5	1508.1	14.859	79.524	78.080	29.30	15.04
5,250	540.43	988.23	2218.1	1763.6	1512.1	14.856	79.637	78.070	29.30	15.01
5,500	539.21	989.78	2219.2	1766.7	1517.7	14.861	79.856	78.313	29.39	14.99
5,750	539.88	991.44	2221.9	1769.9	1523.8	14.867	80.153	78.452	29.46	14.95
6,000	540.41	991.64	2210.0	1771.2	1527.7	14.869	80.421	78.511	29.50	14.95

Table 6.2. Computed temperature and pressure data from MATLAB program in Appendix C.

	T_{t1} [R]	T_{t2} [R]	T_{t4} [R]	T_{t5} [R]	T_{t6} [R]	P_{t1} [psia]	P_{t2} [psia]	P_{t4} [psia]	P_{t5} [psia]	P_6 [psia]
Predicted Value (STP)	520	977.5	2143.6	1715.9	1474.0	14.696	88.623	84.977	30.36	14.98
Measured Value	540.41	991.6	2221.0	1771.2	1527.7	14.869	80.421	78.511	29.50	14.95
% Difference	3.925	1.440	3.611	3.222	3.643	1.177	9.254	7.609	2.842	0.200

Table 6.3. Comparison of predicted to meausred state points.

Measured Parameter	*Engine Model Prediction*	*Superflow System Calculation*	*Computed Values from Measurement Data*
BSFC [lbm/hp-hr]	0.661	0.745	0.620
η_{th}	0.205	0.183	0.210

Table 6.4. Brake specific fuel consumption and thermal efficiency comparisons.

Engine Component	*Engine Model Predicted Power [hp]*	*Superflow System Measured Mechanical Power [hp]*	*Computed Power from Measurement Data [hp]*	*Gearbox Efficiency (η_g) [%]*
Compressor	519.92	-	488.8	-
Gas Generator Turbine	550.56	-	553.5	-
Power Turbine	311.50	242.6	291.2	83.30

Table 6.5. Component Power Comparisons.

Engine Component	*Engine Model Predicted Adiabatic Efficiency [%]*	*Computed Adiabatic Efficiency Based On Measurement Data*
Compressor	74.0%	72% - 73%
Gas Generator Turbine	88.3%	93% - 95%
Power Turbine	85.0%	85.6%

Table 6.6. Component Efficiency Comparisons.

Testing Method	*Temperature(T_{T4}) [R]*	*Percent Difference from Predicted [%]*
Engine Model	2167.0	1.98
Conservation of Energy	2158.3	2.40
Computed Average from Measurement	2210.0	-

Table 6.7. Comparison of GGT inlet temperature.

Designed Test Output Shaft Speed [RPM]	*Actual Output Shaft Speed [RPM]*	*Compressor Efficiency (η_c) [%]*	*GGT Efficiency (η_{ggt}) [%]*	*PT Efficiency (η_{pt}) [%]*	*Compressor Work (W_{comp}) [hp]*	*GGT Work (W_{ggt}) [hp]*	*PT Work (W_{pt}) [hp]*
4,000	4,035	73.13	95.08	75.77	481.7	551.1	254.2
4,250	4,285	73.25	95.14	84.47	477.3	547.1	275.9
4,500	4,533	73.00	93.36	91.98	477.6	540.2	300.1
4,750	4,757	73.14	94.17	89.87	474.5	539.7	290.6
5,000	5,002	73.45	93.07	91.97	477.3	542.7	303.5
5,250	5,251	73.06	94.66	90.14	480.1	553.3	297.4
5,500	5,501	72.57	94.13	88.69	484.5	552.6	295.5
5,750	5,746	72.67	94.05	86.81	488.9	558.9	294.0
6,000	5,995	72.96	93.69	85.66	488.8	553.5	291.2

Table 6.8. Measured thermodynamic engine analysis characteristics from MATLAB program in Appendix C.

Designed Test Output Shaft Speed [RPM]	*Actual Output Shaft Speed [RPM]*	*Fuel-Air Ratio (f)*	*BSFC [lbm/hp-hr]*	*Gearbox Efficiency (η_g) [%]*
4,000	4,035	0.0163	0.7195	83.95
4,250	4,285	0.0161	0.6506	79.20
4,500	4,533	0.0159	0.5902	73.55
4,750	4,757	0.0157	0.6022	76.46
5,000	5,002	0.0159	0.5854	75.61
5,250	5,251	0.0160	0.6001	78.43
5,500	5,501	0.0160	0.6058	80.49
5,750	5,746	0.0160	0.6131	81.96
6,000	5,995	0.0160	0.6198	83.30

Table 6.9. Additional measured thermodynamic engine analysis characteristics from MATLAB program in Appendix C.

Designed Test Output Shaft Speed [RPM]	*Actual Output Shaft Speed [RPM]*	*BSFC [lbm/hp-hr]*	*Shaft Horsepower [hp]*	*Fuel Mass Flow Rate [lbm/hr]*	*Air Flow Rate [CFM]*	*Torque (τ) [lb-ft]*
4,000	4,035	0.8653	213.4	182.9	2502.3	277.8
4,250	4,285	0.8252	218.5	179.5	2489.5	267.8
4,500	4,533	0.8051	220.7	177.1	2492.9	255.6
4,750	4,757	0.7951	222.2	175.0	2491.3	245.3
5,000	5,002	0.7750	229.5	177.7	2508.1	241.0
5,250	5,251	0.7749	233.3	178.5	2507.2	233.3
5,500	5,501	0.7548	237.8	179.0	2508.4	227.0
5,750	5,746	0.7548	241.0	180.3	2527.3	220.3
6,000	5,995	0.7447	242.6	180.5	2530.7	212.5

Table 6.10. Superflow calculated engine performance characteristics.

VII. CONCLUSIONS AND RECOMMENDATIONS

The instrumentation and control of the Allison T63-A-700 gas turbine engine is complete. All temperature and pressure sensing devices from the instrumentation package are functioning with the exception of one thermocouple and one pressure transducer within the thermocouple - pressure ring assembly. Data is being collected by both the data acquisition unit and the dynamometer system. Processing of the collected data for engine performance analysis is accomplished by two separate systems: the Unitek 486 personal computer and the Superflow 901 terminal.

The gas generator turbine and the power turbine speeds are adequately controlled to allow accurate engine cycle analysis and performance calculations for the ME3241 gas turbine laboratory.

All Engineering Operating Procedures have been verified and validated for safe operation of the engine.

Although the control systems and instrumentation package for the gas turbine engine greatly improve the previous ME3241 gas turbine laboratory, there are some areas which require additional study and enhancements. First, the measurement of pressure at the discharge of the compressor needs to be modified to correctly measure the true discharge pressure from the compressor. Second, the gas generator turbine inlet pressure requires the replacement of one pressure transducer in order to obtain a redundant pressure sensor for comparison. Additionally, the gas generator turbine's inlet pressure was found to be slightly lower during testing than predicted by the engine model. Because

the installation of the thermocouple ring assembly required lengthening the engine, a complete check of the air path from the compressor discharge to the gas generator inlet must be conducted to examine for the possibility of air losses from leaks through engine casing. Finally, further testing of the engine must be accomplished in order to accurately map engine performance through all power settings.

It is also recommended that an instrumentation system be designed, fabricated, and installed to monitor vibrations of engine components. The installation manual provides initial guidance in this endeavor and is a good starting point.

Finally, a full maintenance plan must be developed for proper maintenance of the engine instrumentation devices, and support systems. The technical manuals specify periodic maintenance procedures which support increased operating life.

APPENDIX A. MATLAB COMPUTER PROGRAM FOR DETERMINING EFFICIENCY UNCERTAINTY.

```
clear all

%LIST OF VARIABLES
%T1,T2,T3,T4,T5,T6=     Thermodynamic prediticed state point total temperartures
%P1,P2,P3,P4,P5,P6 =    Thermodynamic predicted state point total pressures (psi)
%kc,kg,kp          =    Compressor, GGT, and PT specific heat ratios, respectively
%pi_c,pi_ggt,pi_pt =    Compressor, GGT, and PT pressure ratios, respectively
%tau_c,tau_ggt,tau_pt   =    Compressor, GGT, and PT temperature ratios,
respectively
%t                 =    Temperature Error (F)
%p                 =    Pressure Error (psi)
%upc,upggt,uppt         =    Compressor, GGT, and PT pressure ratio
uncertainty, respectively
%utc,utggt,utpt         =    Compressor, GGT, and PT temperature ratio
uncertainty, respectively
%uncert_c          =    Compressor efficiency uncertainty
%Totunc_cl         =    Low power compressor efficiency uncertainty
%Totunc_ch         =    High power compressor efficiency unertainty
%uncert_ggt        =    GGT efficiency uncertainty
%Totunc_ggtl       =    Low power GGT efficiency uncertainty
%Totunc_ggth            =    High power GGT efficiency unertainty
%uncert_pt         =    PT efficiency uncertainty
%Totunc_ptl        =    Low power PT efficiency uncertainty
%Totunc_pth        =    High power PT efficiency unertainty


%INPUT PARAMETERS BASED ON THERMODYNAMIC CALCULATIONS
T1=[520 520 520 520 520 520 520 520];
T2=[759.4 794.9 831.0 866.7 904 947.6 993 1032.3];
T4=[1401.1 1526.6 1639.2 1743.4 1868.9 2027.6 2202.9 2362.8];
T5=[1155 1249.3 1330.8 1404.8 1499.1 1623.5 1763.5 1893.4];
T6=[1143.9 1211.5 1255 1282.6 1331.3 1409 1507.5 1606.6];
P1=[14.696 14.696 14.696 14.696 14.696 14.696 14.696 14.696];
P2=[42.178 48.931 56.470 64.766 73.927 83.268 91.382 96.365];
P4=[40.184 46.685 53.921 61.872 70.697 79.757 87.666 92.576];
P5=[17.329 19.329 21.384 23.542 26.077 28.795 31.171 32.684];
P6=[14.774 14.761 14.821 14.858 14.900 14.944 14.998 15.032];
kc=[1.4 1.398 1.398 1.397 1.396 1.395 1.394 1.393];
kg=[1.365 1.356 1.350 1.347 1.341 1.335 1.329 1.324];
```

```
kp=[1.365 1.365 1.362 1.359 1.355 1.350 1.344 1.338];


%MOST PROBABLE UNCERTAINTY CALCULATIONS

pi_c =P2./P1;
tau_c=T2./T1;
pi_ggt = P5./P4;
tau_ggt = T5./T4;
pi_pt=P6./P5;
tau_pt=T6./T5;

%%%%%%%%%%%%%%%%%%%%%%
%COMPRESSOR UNCERTAINTY
k=1;
for i = 1:8
    for t=.5:.5:10
        for p = .25:.25:5
            upc=0;
            utc=0;
          upc = pi_c(i) - (P2(i)+p)./P1(i);
          utc =tau_c(i)-(T2(i)+t)./T1(i);
          uncert_c(k)=sqrt(((((kc(i)-1)./kc(i)).*pi_c(i).^...
            (((kc(i)-1)./kc(i))-1))./(tau_c(i)-1).*upc).^2+(-(pi_c(i).^...
            ((kc(i)-1)./kc(i))-1)./((tau_c(i)-1).^2).*utc).^2);
            k=k+1;
          end
    end
end
p=0.25:0.25:5;
t=0.5:0.5:10;
%Low Power Mesh Plot
i=1201;
for j=1:20
    for k = 1:20
        Totunc_cl(j,k)=uncert_c(1,i);
        i=i+1;
    end
end
figure(1);
surf(p,t,Totunc_cl*100);
title('Compressor Uncertainty Analysis N1 Speed = 85%');
xlabel('Pressure Error (psi)')
ylabel('Temp. Error (F)');
```

```
zlabel('Efficiency Uncertainty (%)');
grid;
colorbar;

%High Power Mesh Plot 1
i=2801;
for j=1:20
    for k = 1:20
        Totunc_ch(j,k)=uncert_c(1,i);
        i=i+1;
    end
end
figure(2);
surf(p,t,Totunc_ch*100);
title('Compressor Uncertainty Analysis N1 Speed = 105%');
xlabel('Pressure Error (psi)')
ylabel('Temp. Error (F)');
zlabel('Efficiency Uncertainty (%)');
grid;
colorbar;

%%%%%%%%%%%%%%%%
%GGT UNCERTAINTY
k=1;
for i = 1:8
    for t=.5:.5:10
        for p = .25:.25:5
            upggt=0;
            utggt=0;
                upggt = pi_ggt(i) - (P5(i)+p)./(P4(i)-p);
                utggt =tau_ggt(i)-(T5(i)+t)./(T4(i)-t);
                uncert_ggt(k)=sqrt((utggt*(1/(pi_ggt(i)^((kg(i)-1)/kg(i))-1)))^2+...
                (upggt*(1-tau_ggt(i))*(pi_ggt(i)^((kg(i)-1)/kg(i)))*(kg(i)-1)/...
                ((pi_ggt(i)^((kg(i)-1)/kg(i))-1)^2*kg(i)*pi_ggt(i)))^2);
                k=k+1;
        end
    end
end
p=0.25:0.25:5;
t=0.5:0.5:10;
%Low Power Mesh Plot
i=1201;
for j=1:20
    for k = 1:20
        Totunc_ggtl(j,k)=uncert_ggt(1,i);
```

```
        i=i+1;
    end
end
figure(3);
surf(p,t,Totunc_ggtl*100);
title('GGT Uncertainty Analysis N1 Speed = 85%');
xlabel('Pressure Error (psi)')
ylabel('Temp. Error (F)');
zlabel('Efficiency Uncertainty (%)');
grid;
colorbar;

%High Power Mesh Plot 1
i=2801;
for j=1:20
    for k = 1:20
        Totunc_ggth(j,k)=uncert_ggt(1,i);
        i=i+1;
    end
end
figure(4);
surf(p,t,Totunc_ggth*100);
title('GGT Uncertainty Analysis N1 Speed = 105%');
xlabel('Pressure Error (psi)')
ylabel('Temp. Error (F)');
zlabel('Efficiency Uncertainty (%)');
grid;
colorbar;


%%%%%%%%%%%%%%%%%%%
%POWER TURBINE UNCERTAINTY


k=1;
for i = 1:8
    for t=.5:.5:10
        for p = .25:.25:5
            uppt=0;
            utpt=0;
                uppt = pi_pt(i) - (P6(i)+p)./(P5(i)-p);
                utpt =tau_pt(i)-(T6(i)+t)./(T5(i)-t);
                uncert_pt(k)=sqrt((utpt*(1/(pi_pt(i)^((kp(i)-1)/kp(i))-1)))^2+...
                (uppt*(1-tau_pt(i))*(pi_pt(i)^((kp(i)-1)/kp(i)))*(kp(i)-1)/...
                ((pi_pt(i)^((kp(i)-1)/kp(i))-1)^2*kp(i)*pi_pt(i)))^2);
```

```
                k=k+1;
        end
    end
end
p=0.25:0.25:5;
t=0.5:0.5:10;
%Low Power Mesh Plot
i=1201;
for j=1:20
    for k = 1:20
        Totunc_ptl(j,k)=uncert_pt(1,i);
        i=i+1;
    end
end
figure(5);
surf(p,t,Totunc_ptl*100);
title('PT Uncertainty Analysis N1 Speed = 85%');
xlabel('Pressure Error (psi)')
ylabel('Temp. Error (F)');
zlabel('Efficiency Uncertainty (%)');
grid;

colorbar;

%High Power Mesh Plot 1
i=2801;
for j=1:20
    for k = 1:20
        Totunc_pth(j,k)=uncert_pt(1,i);
        i=i+1;
    end
end
figure(6);
surf(p,t,Totunc_pth*100);
title('PT Uncertainty Analysis N1 Speed = 105%');
xlabel('Pressure Error (psi)')
ylabel('Temp. Error (F)');
zlabel('Efficiency Uncertainty (%)');
grid;

colorbar;
```

APPENDIX B. STANDARD OPERATING PROCEDURES FOR ALIGNMENT AND OPERATION OF THE GAS TURBINE AND DYNAMOMETER TEST SYSTEM

MASTER LIGHTOFF PROCEDURE (MLOP)

SYSTEM VERIFICATION ALIGNMENT PROCEDURES AND OPERATING PROCEDURES

PROCEDURE

PLACING THE GAS TURBINE TEST CELL INTO OPERATION

1. Conduct visual inspection of gas turbine test cell and verify the following:

   a. Ensure all drip pans, piping trenches, and the deck are free of oil, fuel, or any flammable liquids.

   b. Ensure all flammable liquids are stored properly in the flammable liquids locker.

   c. Ensure all small parts, equipment, tools, or objects, which may become airborne debris, are properly stored.

   d. Verify that the gas turbine test cell and work area fire extinguishers are fully charged.

   e. Inspect all piping runs and accessories for loose connections, damage, or leaks.

   f. Ensure all valve handwheels are installed and valve labels are in place.

   g. Inspect the air intake louvers for blockage.

   h. Check the engine battery voltage. Place the batteries on charge if voltage is below 22 VOLTS.

   i. Check fuel level in fuel oil storage tank. Ensure enough fuel is present to support gas turbine operations.

   j. Verify that the water storage tank is full.

2. If the gas turbine test cell and the diesel test cell have been idle for more than 30 days, the water system and fuel system must be recirculated prior to placing the systems into operation. Proceed to the fuel oil service recirculation procedure (FOSRP) and the cooling water system recirculation procedure (CWSRP).

3. If the ambient air temperature is less than 50 °F, the fuel system must be recirculated in order to ensure no paraffin separation is present. Proceed to the fuel oil service recirculation procedure (FOSRP).

4. Ensure the cooling water system filter is clean and free of excessive particulate.

WATER SYSTEM ALIGNMENT

1. Ensure the following valves are in the fully open position:

a. Water storage tank suction valve	CW-1
b. Water supply pump suction valve	CW-2GT
c. Water supply pump discharge valve	CW-4GT
d. Dynamometer sump tank supply valve	CW-6GT
e. Return pump discharge valve	CW-9GT
f. Heat exchanger inlet valve	CW-10
g. Heat exchanger discharge valve	CW-12

2. Ensure the following valves are in the full closed position:

a. Diesel supply pump suction valve	CW-2D
b. Gas turbine to diesel cross connect valve	CW-5
c. Dynamometer bypass valve	CW-7GT
d. Diesel return pump discharge valve	CW-9D
e. Heat exchanger bypass valve	CW-11

f. Dynamometer boost valve CW-12GT

3. Place the local heat exchanger breaker [ ] in the AUTO position.

4. Place the local cooling water supply pump breaker [ ] in the AUTO position.

5. Place the local cooling water return pump breaker [ ] in the AUTO position.

FUEL OIL SYSTEM ALIGNMENT

1. Ensure the following valves are in the fully open position:

   a. Fuel oil supply pump suction valve FOS-2GT

   b. Fuel oil supply pump discharge valve FOS-5GT

   c. Fuel oil supply cell isolation valve FOS-6GT

   d. Fuel oil return valve FOS-12GT

2. Place the local fuel supply pump breaker [ ] in the AUTO position.

3. Ensure the following valves are in the fully closed position:

   a. Diesel fuel oil supply pump suction valve FOS-2D

   b. Fuel oil supply cross-connect valve FOS-3

   c. Fuel oil recirculation valve FOS-9GT

   d. Diesel fuel oil return valve FOS-10D

4. Ensure the dynamometer to engine fuel line quick disconnect is properly connected.

AIR SYSTEM ALIGNMENT

1. Place the remote LOUVER switch to the OPEN position.

2. Ensure air flow turbine meters are connected to the dynamometer instrumentation rack.

3. Remove exhaust covers from gas turbine exhaust stacks.

OIL SYSTEM VERIFICATION

WARNING: *Synthetic lube oil mil-l-23699 can cause dermatitis or paralysis. If lube oil contacts skin, immediately flush with water. If clothing becomes saturated remove promptly.*

1. Verify the lubrication oil level in the oil storage tank is above the fill mark (6 gallon level).

2. Ensure the oil pressure sensing line is connected to the dynamometer instrumentation rack connection.

3. Ensure the oil supply and discharge lines are properly connected to the accessories gearbox.

4. Ensure the shaft is free to turn by rotating manually.

5. Turn on the lubrication oil cooler cooling fan.

ENGINE CHECKS AND ADJUSTMENTS

1. Check gas generator (N1) fuel control lever travel from the control console throttle knob. Ensure full travel from 0 - 90° settings. For full travel lever must contact lever stop. Also ensure that the 0° position actuates the spring fuel cut-off on the governor actuator.

2. Verify the power turbine governor (N2) is lockwired in the MAX position.

3. Ensure all protective covers and plugs are removed from all vents and drains.

4. Ensure the battery charger is disconnected from the storage batteries.

5. Ensure the voltage regulator circuit breaker switch is in the ON position.

6. Obtain the latest barometric reading.

7. Verify the DYNO PRIME switch and the FUEL PUMP switch located on the control console are in the OFF position.

8. Place the LOAD CONTROL switch to the servo position.

9. Ensure the LOAD CONTROL knob is set to 600.

CAUTION: The LOAD CONTROL knob reads one order of magnitude less than order ed speed. Increasing LOAD CONTROL dial indicator above 630 may result in a power turbine overspeed and engine failure.

10. Verify the LOAD CONTROLLING RPM switch is in the LOAD CONTROLLING RPM position. This switch is located inside the control console

11. Place the THROTTLE CONTROL switch in the MANUAL position.

12. Ensure the THROTTLE CONTROL knob is in the fully closed position.

13. Press the POWER ON push-button to energize the dyno control console.

14. Set the shaft OVERSPEED knob at 6,300 RPM.

15. Set the TORQUE/POWER display knob to the LOW scale.

16. Set the SPEED display knob to the LOW speed scale.

17. Adjust the UPPER TEST SPEED knob to 6,250 RPM.

18. Either set the fuel specific gravity knob to the proper setting or input the fuel specific gravity into the SF-901 computer monitoring system in accordance with factory technical manuals.

19. Set the FUEL mode knob to the A configuration.

20. Set the AIR-FUEL meter knob in the AIR/2 configuration.

21. Set the FLOWMETER knob to the 9" position.

22. Set the DISPLAY knob to the TORQUE position.

23. Set the control console switch to the TENTHS scale.

24. Adjust the TORQUE ADJUST knob to zero.

25. Set the DISPLAY knob to the EXHAUST position.

26. Set the water vapor pressure knob to the correct setting.

27. Turn the shutter motor switch [ ] to the OPEN position. Ensure that the intake shutters move to the open position.

28. Ensure both test cell entrance doors are closed and latched.

ENGINE STARTING PROCEDURE

1. Depress the remote COOLING WATER SUPPLY PUMP start push-button [ ]; verify the MOTOR RUN light illuminates.

2. Depress the remote COOLING WATER RETURN PUMP start push-button [ ]; verify the MOTOR RUN light illuminates.

3. Adjust CW-9GT to ensure CW return pump does not become air bound.

4. Depress the remote FUEL OIL PUMP start push-button [ ]; verify the MOTOR RUN light illuminates.

5. Depress the remote HEAT EXCHANGER start push-button [ ]; verify the MOTOR RUN light illuminates.

6. Turn the DYNO PRIME switch to the ON position.

WARNING: *The DYNO PRIME switch must be on for at least 10 seconds prior to engaging starter to ensure the dynamometer has sufficient priming water.*

7. Turn the FUEL PUMP switch to the ON position.

8. Verify both engine test cell doors are closed completely.

9. Depress and hold the STARTER push-button.

10. Verify positive lubrication oil pressure on lube oil pressure gage.

11. Monitor all console warning lights.

12. Advance the gas generator throttle lever (N1) to the 30° (idle position - 6.4V) after N1 speed passes 8,000 RPM (16%).

13. Verify an increase in power turbine speed (N2) by the time N1 speed reaches 20,000 RPM (40%).

14. Monitor turbine outlet temperature. Ensure that TOT does not exceed 1,380 °F for more than ten seconds or 1,700 °F for more than one second.

15. Ensure gas generator speed reaches a steady state idle speed of approximately 31,000 RPM +/- 1,000 RPM (60%).

16. Release the STARTER push-button when N1 is at 31,000 RPM +/- 1,000 RPM.

17. Adjust the servo control LOAD CONTROL knob and manual THROTTLE CONTROL knob as required for engine testing.

WARNING: *Abort start by returning the gas generator THROTTLE CONTROL knob to the 0° position and secure the dynamometer fuel pump if any of the following abnormal conditions occur during system start up:*

1. Time from STARTER push-button depressed to idle speed exceeds one minute.

2. No engine oil pressure is indicated on the control console.

3. Engine oil pressure does not start to increase before N1 speed reaches 10,000 RPM (20%).

4. No indication of power turbine speed N2 before gas generator speed N1 reaches 20,000 RPM (40%).

5. Turbine outlet temperature exceeds 1,380 °F for more than 10 seconds or 1,700 °F for more than one second.

6. A WATER SUPPLY warning light illuminates which indicates a supply water pressure of less tan 15 PSIG is available to the power absorber.

7. A DYNO PRIME warning light illuminates indicating the power absorber must be reprimed.

8. A FUEL PRESSURE warning light illuminates indicating less than 4 PSIG fuel pressure.

9. The OIL PRESSURE warning light illuminates after N1 speed reaches 10,000 RPM (20%).

10. An unusual sound or vibration occurs.

11. A fuel or lubrication oil leak is observed.

FUEL OIL SYSTEM RECIRCULATION PROCEDURE (FOSRP)

PROCEDURE

SYSTEM ALIGNMENT FOR RECIRCULATION

1. Conduct visual inspection of gas turbine test cell and verify the following:

   a. Ensure all drip pans, piping trenches, and the deck are free of oil, fuel, or any flammable liquids.

   b. Ensure all flammable liquids are stored properly in the flammable liquids locker.

   c. Verify that the gas turbine test cell and work area fire extinguishers are fully charged.

   d. Inspect all piping runs and accessories for loose connections, damage, or leaks.

   e. Ensure all valve handwheels are installed and valve labels are in place.

   f. Check fuel level in fuel oil storage tank. Ensure enough fuel is present to support gas turbine operations.

   g. Ensure the intake shutters are closed.

   h. Ensure that the battery charger is disconnected.

2. Ensure the following valves are in the fully open position:

a. Fuel oil supply pump suction valve	FOS-2GT
b. Fuel oil supply pump discharge valve	FOS-5GT
c. Fuel oil supply cell isolation valve	FOS-6GT
d. Fuel oil recirculation valve	FOS-9GT
f. Fuel oil return valve	FOS-12GT

3. Ensure the fuel oil service flow regulator is adjusted between 6-10 PSIG.

4. Ensure the following valves are in the fully closed position:

   a. Diesel fuel oil supply pump suction valve FOS-2D

   b. Fuel oil supply cross-connect valve FOS-3

   c. Diesel fuel oil return valve FOS-10D

5. Place the local fuel oil supply pump breaker [ ] in the AUTO position.

6. Turn the remote fuel oil pump breaker [ ] to the ON position.

7. Monitor system for possible leaks.

NOTE: The system will recirculate and filter fuel at a rate of 60 gallons per hour. The total storage tank capacity is 500 gallons.

COOLING WATER SYSTEM RECIRCULATION PROCEDURE (CWSRP)

PROCEDURE

SYSTEM ALIGNMENT FOR RECIRCULATION

1. Conduct visual inspection of gas turbine test cell and verify the following:
   a. Inspect all piping runs and accessories for loose connections, damage, or leaks.
   b. Ensure all valve hand wheels are installed and valve labels are in place.
   c. Verify that the water storage tank is full.
   d. Ensure the cooling water system filter is clean and free of excessive particulate.

2. Ensure the following valves are in the fully open position:

a. Water storage tank suction valve	CW-1
b. Water supply pump suction valve	CW-2GT
c. Water supply pump discharge valve	CW-4GT
d. Dynamometer bypass valve	CW-7GT
e. Heat exchanger bypass valve	CW-11
f. Dynamometer boost valve	CW-12GT

3. Ensure the following valves are in the fully closed position:

a. Diesel supply pump suction valve	CW-2D
b. Gas turbine to diesel cross connect valve	CW-5
c. Dynamometer sump tank supply valve	CW-6GT
d. Diesel return pump discharge valve	CW-9D
e. Return pump discharge valve	CW-9GT

f. Heat exchanger inlet valve CW-10

g. Heat exchanger discharge valve CW-12

4. Place the local cooling water supply pump breaker [ ] in the AUTO position.
5. Monitor system and check for leaks.

NOTE: The water will recirculate at 50 gallons per minute. A full tank will recirculate once every 20 minutes. It is recommended that the system be placed into recirculation mode for a minimum of 40 minutes if the system has been idle more than 30 days.

MASTER NORMAL SHUTDOWN PROCEDURE (MNSP)

PROCEDURE

NORMAL ENGINE AND DYNAMOMETER SHUTDOWN PROCEDURES

1. Return the gas generator control lever (N1) to the IDLE position 30,000- 32,000 RPM (60%).

2. Adjust the manual LOAD CONTROL knob to read 8 volts on the TEMPERATURE VOLT meter scale.

3. Allow the engine to run at idle for two minutes to facilitate a sufficient engine cool down.

4. Return the gas generator throttle control to the 0° (cut-off) position.

5. Turn dynamometer FUEL PUMP OFF and monitor for decrease in N1 speed and turbine outlet temperature (TOT).

NOTE: If N1 speed fails to decrease, secure remote fuel oil pump breaker [ ] and monitor N1 speed.

If TOT temperature does NOT decrease and N1 speed does decrease, a post shutdown fire exists. Depress STARTER push-button and motor engine for two minutes.

5. Turn the remote fuel oil supply pump breaker [ ] to the OFF position.

6. Turn the remote cooling water supply pump breaker [ ] to the OFF position.

7. Turn the remote cooling water return pump breaker [ ] to the OFF position.

8. Turn the remote heat exchanger breaker [ ] to the OFF position.

9. Return all local power panel breakers to the OFF position.

10. Depress the POWER ON push-button to de energize the dynamometer control console.

11. Turn off the oil cooler cooling fan.

12. Close the following valves:

a. Fuel oil supply suction valve	FOS-2GT
b. Fuel oil supply pump discharge valve	FOS-5GT
c. Fuel oil return valve	FOS-12GT
d. Water storage tank suction valve	CW-1
e. Water supply pump suction valve	CW-2GT
f. Return pump discharge valve	CW-9GT

13. Ensure all protective covers and plugs are repositioned on all vents and drains.

14. Turn the remote shutter motor breaker [ ] to the CLOSE position. Ensure that the intake shutters move to the closed position.

15. Turn off the installed cell cooling fans from the wall mounted thermostat when the cell is sufficiently ventilated.

EMERGENCY SHUTDOWN PROCEDURE (ESP)

IMMEDIATE AND CONTROLLING ACTIONS FOR EMERGENCY SHUTDOWN OF THE GAS TURBINE TEST CELL.

NOTE: Emergency shutdown of the T63-A-700 gas turbine engine and dynamometer is directed for any one or combinations of the following casualties:

a. A WATER SUPPLY warning light illuminates which indicates a supply water pressure of less than 15 PSIG is available to the power absorber.

b. A DYNO PRIME warning light illuminates indicating that the power absorber has lost prime.

c. A FUEL PRESSURE warning light illuminates indicating that there is less than 4 PSIG fuel pressure.

d. A fuel oil leak occurs.

e. A WATER TEMP. warning light illuminates indicating a power absorber cooling water discharge temperature of over 210 °F. A normal shutdown should be initiated IAW EOP MNSP if a cooling water discharge of 160 °F or above is observed.

f. An oil pressure of less than 60 PSIG is observed, an automatic shutdown should occur if an oil pressure less than 50 PSIG occurs.

g. An oil leak occurs.

h. An unusual metallic or vibrational sound occurs.

i. The overspeed warning light is illuminated.

j. A fire of any type or severity is observed.

k. A gas generator overspeed of 53,164 RPM (104%) is observed.

l. A power turbine overspeed of 36,400 RPM (104%) is observed.

m. A compressor stall is observed.

n. Erratic control console readings occur.

o. Uncontrolled dyno load fluctuations occur.

p. A turbine outlet temperature (TOT) of 1,380 °F for more than 10 seconds occurs.

q. A TOT of 1,700 °F occurs.

r. An oil temperature of 225 °F or above is observed.

PROCEDURE

1. Turn the dynamometer FUEL PUMP OFF and return the gas generator throttle control to the 0° (cut-off) position. Monitor for a decrease in N1 speed and TOT temperature.

NOTE: If N1 speed fails to decrease, secure remote fuel oil pump breaker [ ] and monitor N1 speed.

If TOT temperature does NOT decrease and N1 speed does decrease, a post shutdown fire exists. Depress STARTER push-button and motor engine for two minutes.

2. After N1 speed reaches 0 RPM (0%) proceed with normal shutdown IAW SOP MNSP.

NOTE: In the event of a fire, call the fire department at extension 2333.
Attempt to put out fire with CO_2 extinguisher only after calling fire department.

3. **Troubleshoot and investigate malfunction prior to attempting a restart of the engine.**

APPENDIX C. MATLAB COMPUTER PROGRAM USED TO DETERMINE ENGINE PERFORMANCE CHARACTERISTICS.

```
%This m-file computes various performance characteristics  for a T63-A-700 Gas Tubine
%Engine.


%User Inputed Data

clear all
data = input('Enter the file name of the saved data for engine analysis:  ','s')
n = input('Enter the number of data runs taken for your tests: ')
correct = input('Enter Atmospheric Pressure [in. Hg]:  ')
Qa = input('Enter the vector of air flow rates [CFM]: ')
mf = input('Enter the vector of fuel mass flow rates [lbm/hr]: ')
power = input('Enter the vector of the Superflow Computed SHP [hp]: ')
speed = input('Enter the vector of output shaft speed as recorded Superflow: ')
sfc = input('Enter the vector of SFC values as computed by the Superflow system: ')
load data
data(1:60,1:n)=data(1:60,1:n)+460;
correct = correct*.49115;
R=53.3;                                          %Gas Constant [ft-lbf/lbm-R]

%Check for Bad Thermocouples
num = size(data(:,1));
for i=1:num(1)
        for j = 1:n
                if data(i,j) > 3000
                        data(i,j) = (data(i-1,j) + data(i-2,j) +data(i+1,j) +data(i+2,j))/4;
                end
        end
end
i=1;
r0=2.57
r1=2.985
r2=3.075
r3=3.18

%Pressure and Temperature Computation

for i= 1:n
Tt1(i)=sum(data(1:2,i))/2;                       %Compressor inlet total temp.
Tt2(i)=data(4,i);                                %Compressor outlet total temp.
T1(i)=sum(data(5:20,i))/16;                      %Inner t-couple average temp
T2(i)=sum(data(21:36,i))/16;                     %Middle t-couple average temp
```

```
T3(i)=sum(data(37:52,i))/16;                    %Outer t-couple average temp
cp = [4.87e-12 -2.301387e-8 5.726375972e-5 .21166288614250];
cp_1(i) = polyval(cp,T1(i));
cp_2(i) = polyval(cp,T2(i));
cp_3(i) = polyval(cp,T3(i));
cp_av(i)=(cp_3(i)+cp_2(i)+cp_1(i))/3;           %GGT inlet total temp.
Tt4(i) = ((r3^2-r2^2)*T3(i)*cp_3(i) + (r2^2-r1^2)*T2(i)*cp_2(i) + (r1^2-
r0^2)*T1(i)*cp_1(i))/((r3^2-r0^2)*cp_av(i));
Tt5(i) = data(53,i);                            %PT inlet total temp.
Tt6(i) = sum(data(54:57,i))/4;                  %PT outlet total temp.

Pt1(i) =data(61,i)+correct;                     %Comp. inlet total pressure
Pt2(i) =data(62,i)+correct;                     %Comp. discharge total pressure
Pt4(i) =sum(data(64,i))+correct;                %GGT inlet total pressure
Pt5(i) =sum(data(66:67,i))/2+correct;           %PT inlet total pressure
P6(i) = sum(data(68:69,i))/2+correct;           %PT exhaust static pressure
end

%Pressure and Temperature Ratios
pi_c = Pt2./Pt1;                                %Comp. pressure ratio
pi_ggt = Pt5./Pt4;                              %GGT pressure ratio
pi_pt = P6./Pt5;                                %PT pressure ratio
tau_c = Tt2./Tt1;                               %Comp. temp. ratio
tau_ggt = Tt5./Tt4;                             %GGT temp. ratio
tau_pt = Tt6./Tt5;                              %PT temp. ratio



%Specific heat and Specific heat ratio calculated
Tcomp = ((Tt1 + Tt2)/2);
Tggt = ((Tt5 + Tt4)/2);
Tpt = ((Tt5 +Tt6)/2);
cp = [4.87e-12 -2.301387e-8 5.726375972e-5 .21166288614250];
k = [-1.63e-12 1.397353e-8 -7.840417412e-5 1.44508089202454];
cp_comp = polyval(cp,Tcomp);
cp_ggt = polyval(cp,Tggt);
cp_pt = polyval(cp,Tpt);
k_comp = polyval(k,Tcomp);
k_ggt = polyval(k,Tggt);
k_pt = polyval(k,Tpt);

%Component Efficiency Calculations
nc = (pi_c.^((k_comp-1)./k_comp)-1)./(tau_c-1)          %Compressor
nggt= (1-tau_ggt)./(1-pi_ggt.^((k_ggt-1)./k_ggt))       %GGT
```

```
npt= (1-tau_pt)./(1-pi_pt.^((k_pt-1)./k_pt))                %PT



%Power for Each Component
ma= Qa.*(Pt1./(R*Tt1))*144/60;                              %Air mass flow [lbm/sec]
mf = mf/3600;                                               %Fuel mas flow [lbm/sec]
Wc = 1.4148*ma.*cp_comp.*(Tt2-Tt1)                          %Comp. Work [hp]
Wggt =1.4148*(ma +mf).*cp_ggt.*(Tt4 - Tt5)                  %GGT Work [hp]
Wpt = 1.4148*(ma +mf).*cp_pt.*(Tt5-Tt6)                     %PT Work [hp]

%Other Calculations
f = mf./ma                                                  %Air-Fuel Ratio
BSFC = mf*3600./Wpt                                         %Fuel Consumption
ng = power./Wpt                                             %Gear Box Efficiency

%Graphical representation
figure(1)
plot(speed,Wpt,'r',speed,power,'g')
title('Power Turbine Work and Measured Mechanical Work')
xlabel('Output Shaft Speed [RPM]')
ylabel('Power [hp]')
grid
c=legend('Thermodynamic Power Turbine Work','Superflow Measure Mechanical Work')
axes(c)

figure(2)
plot(speed,BSFC,'r',speed,sfc,'g')
title('Specific Fuel Consumption')
xlabel('Output Shaft Speed [RPM]')
ylabel('BSFC [lb/hp-hr]')
grid
b=legend('Thermodynamic SFC', 'Superflow SFC')
axes(b)

figure(3)
plot(speed,nc,'r',speed,nggt,'g',speed,npt,'b')
grid
title('Components Adiabatic Efficiency vs. Engine Speed')
xlabel('Output Shaft Speed [RPM]')
ylabel('Efficiency [%]')
grid
a=legend('Compressor','Gas Generator Turbine','Power Turbine')
axes(a)
```

LIST OF REFERENCES

1. Allison Gas Turbines, *Model-C18 Installation Design Manual*, 1976.

2. Kline, S. J., McClintock, F. A., *Describing Uncertainties in Single-Sample Experiments*, Mechanical Eng. 75: 3-8, January 1953.

3. Beckwith, Thomas G., Marangoni, Roy D., and Lienhard V, John H., *Mechanical Measurements*, pp. 637-638, Addison-Wesley Publishing Company, 1993.

4. Point of Contact Adam Rakiey, President, United Sensor Corporation - 3 Northern Boulevard, Amherst, NH, 03031-2329, PH: (603) 672-0909, April 1996.

5. White, Frank M., *Fluid Mechanics*, pp.270-272, McGraw-Hill, Inc., 1994.

6. Meirovitch, Leonard, *Elements of Vibration Analysis*, p. 226, McGraw-Hill, Inc., 1986.

7. Eckerle, Brian P., *Design and Component Integration of a T63-A-700 Gas Turbine Engine Test Facility*, September 1995.

8. Point of Contact Tom Christian, Electronic / Computer systems engineer, Naval Postgraduate School - Code ME/CS, 700 Dyer Road, Monterey, CA 93943-5100, PH: (408) 656-3208, April 1996.

9. Point of Contact Bill Shealy, Lori Corporation, Customer Service Representative, 6930 North Lakewood, Tulsa, OK 74101, PH (918) 272-8000, March 1996.

10. Point of Contact Tom Magin, Niagara Development and Manufacturing Company, Customer Service Representative, 3315 Haseley Drive, Niagara Falls, NY 14304, PH (716) 297-0652.

11. Point of Contact Tim Hillstrum, Allison Engine Corporation, Design Engineer, P.O Box 420, Indianapolis, IN 46206-0420, PH (317) 230-4515.

INITIAL DISTRIBUTION LIST

	No. of copies
1. Defense Technical Information Center 8725 John J. Kingman Rd. STE 0944 Alexandria, Virginia 22304-6145	2
2. Dudley Knox Library Naval Postgraduate School 411 Dyer RD. Monterey, California 93943-5101	2
3. Department Chairman, Code ME Department of Mechanical Engineering Naval Postgraduate School Monterey, California 93943-5000	1
4. Professor Knox T. Millsaps Code ME/Ps Department of Mechanical Engineering Naval Postgraduate School Monterey, California 93943-5004	3
5. Curricular Officer, Code 34 Department of Mechanical Engineering Naval Postgraduate School Monterey, California 93943-5100	1
6. Mr. Tim Hillstrom Allison Engine Co. P.O. Box 420 Indianapolis, Indiana 46206-0420	1
7. Mr. Bill Shealy LORI Co. 6930 North Lakewood Tulsa, OK 74101-3629	1
8. Mr. Tom Magin Niagara Development and Manufacturing Co. 3315 Haseley Drive Niagara Falls, NY 14303	1

9. Mr. Daniel Haas — 1
Walsh - Pacific Construction
299 Foam Street
Monterey, CA 93940

10. Mr. Barry Haas — 1
110 Springs Cove
Boulder, CO 80027

11. Mr. Adam Rakeiy — 1
United Sensor Corporation
3 Northern Boulevard
Amherst, NH 03031-2329

12. LT David W. Haas,USN — 2
110 Springs Cove
Boulder, Colorado 80027